October 2021

Structure-Function Studies of the Trypanosome Mitochondrial Replication Protein POLIB

Raveen Armstrong
University of Massachusetts Amherst

STRUCTURE-FUNCTION STUDIES OF THE TRYPANOSOME MITOCHONDRIAL REPLICATION PROTEIN POLIB

A Thesis Presented

by

Raveen Armstrong

Submitted to the Graduate School of the
University of Massachusetts Amherst in partial fulfillment
of the requirements for the degree of

MASTER OF SCIENCE

September 2021

Department of Microbiology

STRUCTURE-FUNCTION STUDIES OF THE TRYPANOSOME MITOCHONDRIAL REPLICATION PROTEIN POLIB

A Thesis Presented

by

Raveen Armstrong

Approved as to style and content by:

DocuSigned by:
92DFBACA724F4C0...
Michele M. Klingbeil, Chair
Department of Microbiology

DocuSigned by:
7FB831114FBC40C...
Yasu S. Morita, Member
Department of Microbiology

DocuSigned by:
5FB844312DE0492...
Klaus Nusslein, Member
Department of Microbiology

DocuSigned by:
1F0CE8945AD74BE...
James F. Holden, Department Head
Department of Microbiology

DEDICATION

This thesis is dedicated to my family who provided me with constant support, encouragement, and love throughout this journey of mine.

I would like to thank my friends in Bangalore, India for the fond memories and for always being there for me.

I also dedicate this to all the teachers and mentors who have inspired and influenced me to become the person I am today.

I am also thankful to all the people who discouraged me when I was trying to pursue a career in the life sciences, because you pushed me to discover what I am really meant to do.

Thank you.

ACKNOWLEDGEMENTS

I am extremely grateful to my advisor and mentor Prof. Michele Klingbeil for providing me with the opportunity to pursue my thesis research in her laboratory. It has been an incredible experience learning from her and growing as a researcher. She has pushed me to a higher level of excellence with respect to critical thinking, discipline, and organization.

I am thankful to all the members of the Klingbeil lab who I've had an opportunity to interact with and for having provided me with valuable advice when needed: Stephanie Delzell, Maira Ahmed, Tal Taylor, Brendan Maher, Annie Yang and John Micue.

I would also like to thank the members of my committee for their contributions and cooperation throughout this process.

I thank every person in UMass Amherst who in some way or the other helped me get closer to achieving my goals.

Last but not the least, my heartfelt gratitude goes out to my parents for believing in me and supporting me financially during my time here.

ABSTRACT

STRUCTURE-FUNCTION STUDIES OF THE TRYPANOSOME MITOCHONDRIAL REPLICATION PROTEIN POLIB

SEPTEMBER 2021

RAVEEN ARMSTRONG, B.TECH PES UNIVERSITY

M.S. UNIVERSITY OF MASSACHUSETTS AMHERST

Directed by: Dr. Michele M. Klingbeil

Trypanosoma brucei and related protists are distinguished from all other eukaryotes by an unusual mitochondrial genome known as kinetoplast DNA (kDNA) that is a catenated network composed of minicircles and maxicircles. Replication of this single nucleoid involves a release, replicate, and reattach mechanism for the thousands of catenated minicircles and requires at least three DNA polymerase (*POLIB*, *POLIC* and *POLID*) with similarity to *E. coli* DNA polymerase I. Like other proofreading replicative DNA polymerases, *POLIB* has both an annotated polymerase domain and an exonuclease domain. Predictive modelling of *POLIB* indicates that it has the canonical right hand polymerase structure with a unique and large 369 amino acid insertion within the polymerase domain (thumb region) homologous to *E. coli* RNase T. The goal of this study was to evaluate whether the polymerase domain is necessary for the essential replicative role of POLIB**.** To study the structure-function relationship, an RNAi-complementation system was designed to ectopically express *POLIB* variants in *T. brucei* that has endogenous *POLIB* silenced by RNAi.

Control experiments expressing an ectopic copy of *POLIB* wildtype (IBWT^{PTP}) or polymerase domain mutant (IBPol-^{PTP}) in the absence of RNAi did not impact fitness in procyclic cells despite protein levels being 5 - 8.5 fold higher than endogenous POLIB levels. Immunofluorescence detection of the tagged variants indicated homogenous expression of the variants in a population of cells and negligible changes in kDNA morphology. Lastly, Southern blot analyses of cells expressing the IBWT^{PTP} or IBPol-^{PTP} variants indicated no changes in free minicircle species.

A dually inducible RNAi complementation system was designed and tested with the IBWT^{PTP} and IBPol-^{PTP} variants. Inductions of *POLIB* RNAi accompanied by ectopic expression of either variant using the standard 1 μg/ml tetracycline resulted in low protein levels of both variants while knockdown of the endogenous *POLIB* mRNA was greater than 85%. Increasing the tetracycline concentration to 4 μg/ml improved expression levels of both variants. However, levels of the ectopically expressed variants never exceeded that of endogenous POLIB. Using the 4 μg/ml induction conditions, complementation with IBWT^{PTP} resulted in a partial rescue of the POLIB RNAi phenotype based on fitness curves, quantification of kDNA content and Southern blot analysis of free minicircles. IBWT^{PTP} complementation resulted in gradual increase of IBWT^{PTP} protein levels over the 10 day induction, and a small kDNA phenotype instead of the progressive loss of kDNA normally associated with *POLIB* RNAi. Additionally, the loss of free minicircles was delayed.

Complementation with the IBPol-^{PTP} variant produced more consistent levels of IBPol-^{PTP} protein although still below endogenous POLIB levels. Loss of fitness was similar to *POLIB* RNAi alone. However, a small kDNA phenotype emerged early after just four days of complementation and persisted for the remainder of the induction. The majority of the IBRNAi + IBPol-^{PTP} population (70%) contained small kDNA compared to the parental *POLIB* RNAi or IBWT^{PTP} complementation that had only 45% and 50% small kDNA, respectively. Lastly, the pattern of free minicircle loss closely resembled POLIB RNAi alone. Together, these data suggest that the dually inducible system results in a partial rescue with the IBWT^{PTP} variant. Rescue with IBPol-^{PTP} variant results in a noticeably different phenotype from either *POLIB* RNAi alone or IBWT^{PTP} complementation indicating that the POLIB polymerase domain is likely essential for the *in vivo* role of POLIB during kDNA replication.

TABLE OF CONTENTS

Page

LIST OF FIGURES

CHAPTER 1

INTRODUCTION

Towards the end of the 20th century, the evolutionary biologist Lynn Margulis advanced the serial endosymbiotic theory of mitochondrial origin. She hypothesized that the eukaryotic cell organelles-mitochondria, plastids and the basal bodies of the flagella have a prokaryotic origin (Sagan, 1967). This comprehensive symbiotic view of eukaryotic evolution is considered one of the first unified theories of eukaryogenesis (Gray, 2017). The proposed endosymbiotic origin of mitochondria and plastids were widely accepted and is now firmly established, however her hypothesis about the eukaryotic flagella could not be directly tested and was dismissed. The simple reason being that no genome was associated with the eukaryotic flagellum despite efforts to find one (Johnson and Rosenbaum, 1991).

Organellar genomes contain genes for respiration (mitochondria), photosynthesis (plastids), and even the construction of their own ribosomes (Clark et al., 2019). Considering their vital roles, it seems important that they are accurately and efficiently replicated so that the genetic information is maintained and faithfully transmitted. These organellar genomes are duplicated by dedicated replication machinery, which includes a replicative DNA polymerase in addition to DNA repair enzymes. Amongst the eukaryotic lineages, taxons use different DNA polymerases to replicate their organelle whether it is a mitochondrion or a plastid (Figure 1A). While Opisthokonts use mitochondrial DNA polymerase γ, two Plant Organellar Polymerases (POP) are distributed among taxa that have mitochondria and chloroplasts. Mitochondria are semi-autonomous organelles containing their own genome and encoding genes necessary for a myriad of functions like oxidative phosphorylation. They are also involved in the regulation of signaling pathways, cell death and cell proliferation through cross-talk with the nuclear genome (Whelan and Zuckerbraun, 2013). The structural divergence and intricacies amongst mitochondria and their extra-nuclear genomes in eukaryotes are baffling. Much of this diversity is found within the kingdom Protoctista (Corliss, 1989). For example, the three major lineages of the phylum

Euglenozoa: Euglenida, Diplonemea and Kinetoplastida have very differently organized mitochondrial genomes (Figure 1B). Euglenida possess linear mitochondrial DNA molecules of variable length while Diplonemea and Kinetoplastida contain circular DNA molecules in different arrangements.

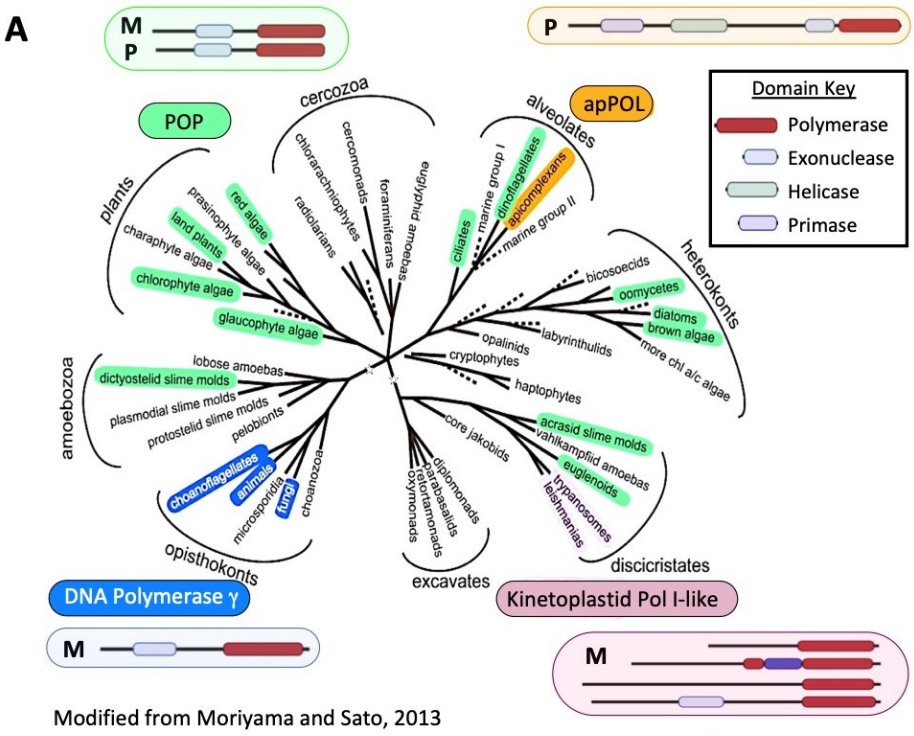

Modified from Moriyama and Sato, 2013

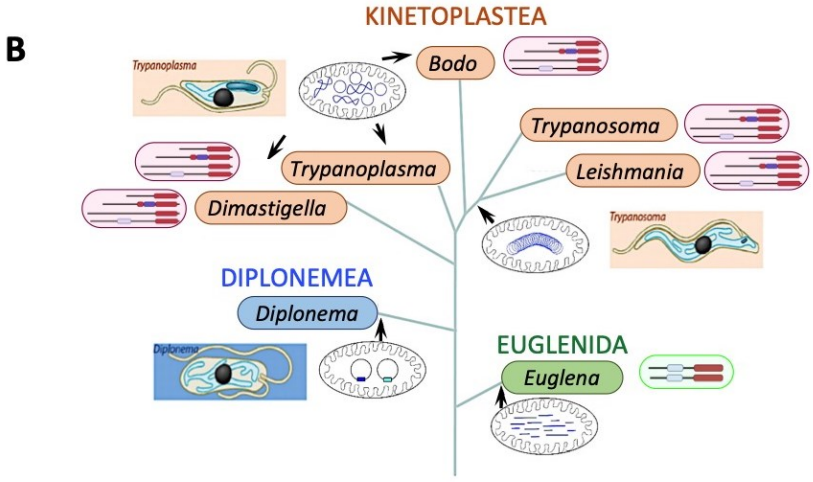

Modified from Kaufer et al., 2020 and Lukes et al., 2018.

Figure 1: Eukaryotic Phylogenetic Relationship
A) Distribution of Family A DNA polymerases in eukaryotes overlaid on a consensus eukaryotic tree. Plant Organellar Polymerases (green), Animal DNA Polymerase γ (blue), Apicomplexan replication-repair Polymerase (orange), and Kinetoplastida Pol I-like DNA polymerases (magenta)
B) Schematic phylogenetic tree of life representing Euglenozoa. Different organization of their mitochondrial genomes (in blue) is shown for the three major lineages: Kinetoplastea (in orange), Diplonemea (in blue), and Euglenida (in green).

Kinetoplastid parasites are some of the earliest diverging eukaryotes to have retained their mitochondria. These flagellated protists have the best studied non-nuclear genome and comprise of a divergent group of free living and parasitic eukaryotes which contain relaxed and/or catenated mitochondrial DNA molecules (Lukeš et al., 2018). Trypanosomatids are studied extensively due to their significant medical and economic relevance (Boelaert et al., 2010). Their mitochondria contain a network of thousands of interlocked circular DNA molecules called maxicircles and minicircles that are condensed into a disk like structure (Lukeš et al., 2010). The complexity of their mitochondrial genomes and the processes involved in replicating it alludes to the involvement of expanded families of mitochondrial DNA polymerases.

Trypanosoma brucei is the causative agent of the fatal Human African Trypanosomiasis (HAT) and Nagana, a wasting disease in livestock. A complicating feature is the several subspecies of *T. brucei* that cause differing disease in mammals. *T. brucei brucei* is strictly an animal pathogen because humans produce trypanosome lytic factor to combat this subspecies (Raper et al., 1999). *T. brucei rhodesiense* and *T. brucei gambiense* are resistant to the lytic factor causing different forms of the fatal human disease. While infections with *T. b. rhodesiense* can kill within weeks to months, the *gambiense* subspecies cause chronic disease that takes years between infection and death (Burri et al., 2004). The currently available drugs to treat have high toxicity and are difficult to administer in endemic regions where this is prevalent (Baral, 2010). Not only is this a public health issue in such regions but also one that leads to severe economic losses in the agricultural industry (Hotez, 2008; Hotez et al., 2012). Trypanosomes have a digenetic lifestyle, where mammals act as the definitive host while an arthropod vector called the tsetse fly acts as the intermediate host (Dyer et al., 2013).

Additionally, *Trypanosoma brucei rhodesiense* has many animal reservoirs, thereby making it nearly impossible to eradicate (Njiokou et al., 2006; Simo et al., 2006). Exploiting unique biological features and molecular mechanisms is the best way to find new druggable targets.

Housed in the single mitochondrion of the parasite is a network of catenated circular DNA molecules called the kinetoplast DNA (kDNA) (Shlomai, 2004). This is considered the most complex mitochondrial DNA found in nature. This network replicates once per cell cycle and in near synchrony with nuclear S phase through an elaborate, yet coordinated mechanism of release, replication, and reattachment of minicircles, while the maxicircles replicate attached to the network (Woodward and Gull, 1990; Jensen and Englund, 2012) (Figure 2). Covalently closed minicircles are released vectorially from the network into the kinetoflagellar zone (KFZ), a region between the kDNA disk and the basal body (Drew and Englund, 2001). In the KFZ, the minicircles undergo unidirectional replication via theta structures (early events). The progeny minicircles containing gaps migrate to the antipodal sites to undergo Okazaki fragment processing with the help of other proteins (later events). During the final stages, the minicircle progeny get attached to the network and the gaps are repaired (Hines et al., 2001; Melendy et al., 1988). At least 6 DNA polymerases are involved in kDNA transactions, where three are Family A DNA polymerases (POLIB, POLIC and POLID) and play non-redundant roles in kDNA replication (Klingbeil et al., 2002; Saxowsky et al., 2003; Chandler et al., 2008; Bruhn et al., 2011). The presence of these paralogs suggests that these proteins may have evolved specialized functions in kDNA replication.

Like other proofreading replicative DNA polymerases, POLIB has both an annotated polymerase domain and an exonuclease domain (Figure 3A), and protein alignments indicate conservation of three highly conserved motifs in the polymerase and exonuclease domains including the catalytic Asp residues (data not shown). Previous research in the lab, established that *POLIB* is essential for minicircle replication using RNA interference (Klingbeil et al., 2002; Bruhn et al., 2010; Bruhn et al., 2011). Depletion of *POLIB* by RNAi resulted in loss of fitness (LOF), a decrease in both minicircle and maxicircle copy number, and progressive loss of the kDNA network; hallmarks of a kDNA replication defect. Yet, a role in maxicircle replication was never addressed.

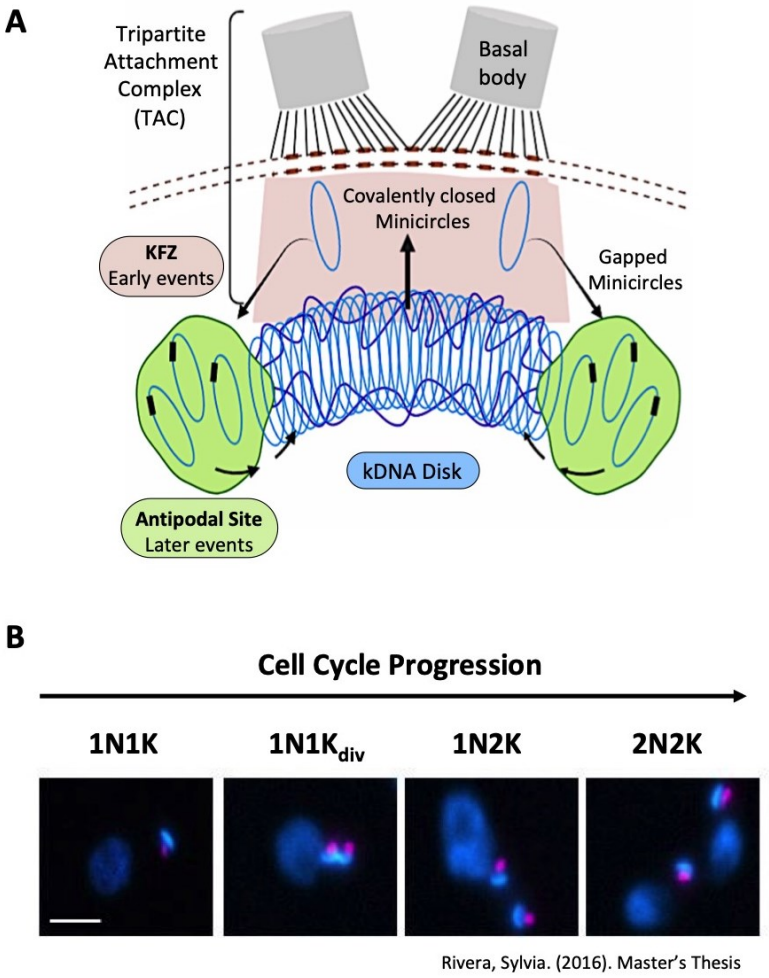

Figure 2: Kinetoplast DNA replication in *Trypanosoma brucei.*
A) Model of kDNA replication. See details in text of Introduction. **B)** Representative images of different stages of cell cycle in *Trypanosoma brucei brucei*. DAPI staining (blue) indicates the larger nucleus (N) and kDNA nucleoid (K), Magenta indicates basal bodies. Size bar, 5 μM.

Homology modelling of *POLIB* indicates that it has the conventional right hand polymerase structure, and a 369 aa insertion in the thumb domain resembling RNase T, belonging to DnaQ superfamily of exonucleases (Figure 3B). This feature of *POLIB* is unique among all Family A polymerases studied thus far, and likely contributes to a specialized role in kDNA replication. The overall goal of this project is to understand the independent roles of the annotated domains. A genetic complementation approach was used wherein inducible expression of dsRNA to knockdown the *POLIB* gene was coupled with ectopic overexpression of wild type and a polymerase domain mutated variant.

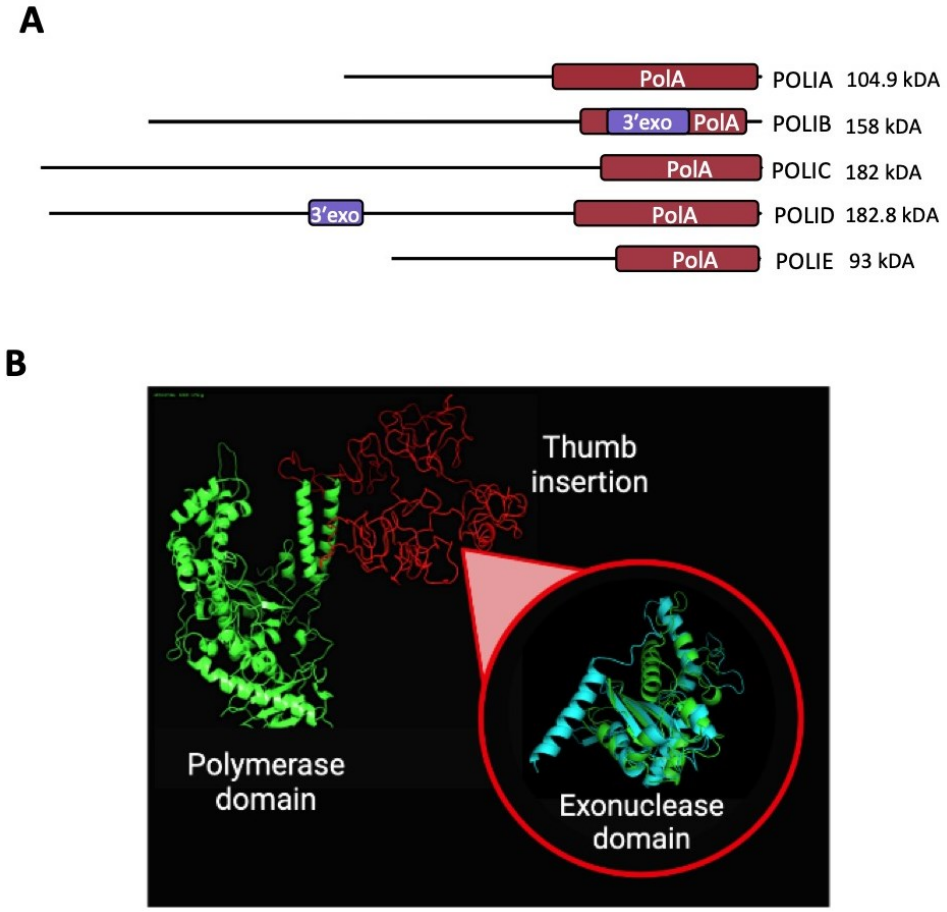

Figure 3: Unique features of POLIB.
A) Schematic comparison of protein domains of the *Trypanosoma brucei* family A DNA polymerases. The colored boxes indicate domains predicted from Pfam database: red, polymerase domain; blue, 3′- 5′ exonuclease domain. B) Homology model of *TbPOLIB* acquired by Phyre2. Amino acids 441-1365. The thumb insertion was modeled on RNAse T amino acids 660-1030.

The complementation system is a dual-function TET-ON system that can be used to simultaneous induce dsRNA to deplete a gene and co-express a copy of a protein ectopically. It is comprised of an integrated RNAi vector and a protein-expression plasmid integrated into the ribosomal DNA spacer region of the trypanosomes (Figure 4). Expression of the dsRNA is driven by a *T. brucei* procyclin promoter and is regulated by two tetracycline operator sequences bound by repressor. Addition of tetracycline allows derepression and transcription. The protein-expression plasmid contains a strong T7 promotor upstream of just a single tetracycline operator sequence. This dual expression system was used to establish the complementation system, determine the contribution of the polymerase domain and test whether it is

essential *in vivo*. POLIB with a mutated polymerase domain is unable to rescue the loss of fitness caused by depleting endogenous POLIB in the cell. Data obtained from microscopy and Southern blot experiments point to a kDNA replication defect. We present data that the polymerase domain is an essential part of POLIB and possibly contributes to the overall function *in vivo*.

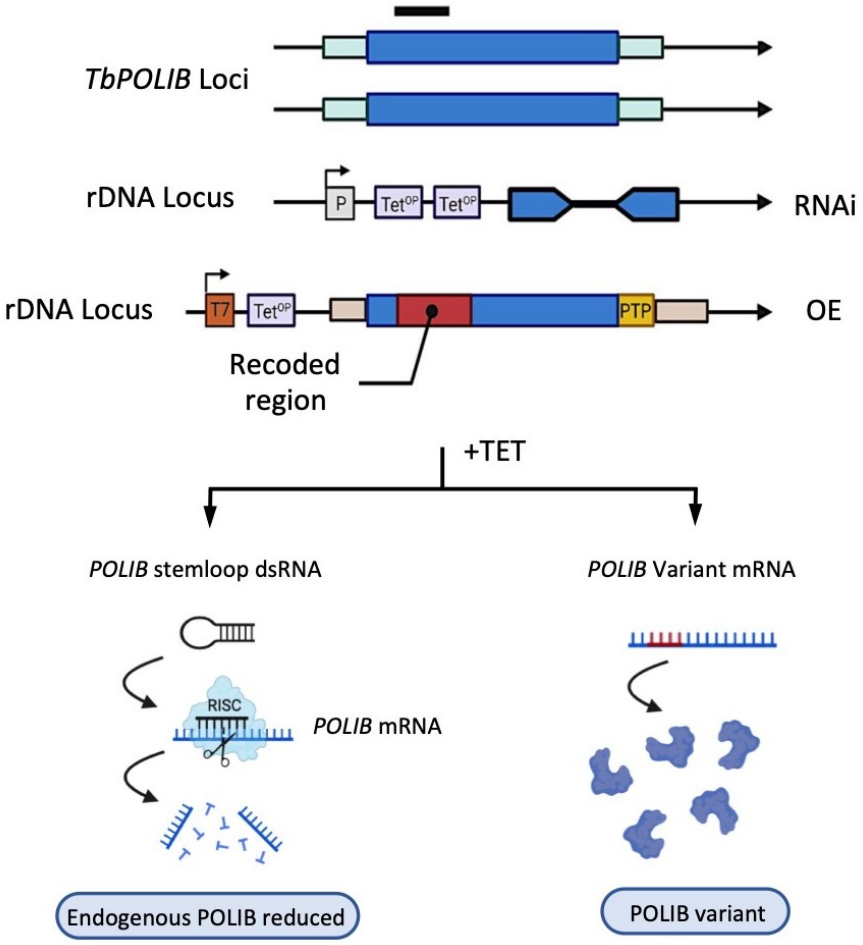

Figure 4: Schematic representation of the RNAi complementation system used in *Trypanosoma brucei brucei* 29-13 procyclic cells.

This dually inducible system can be used to produce a stemloop dsRNA trigger to deplete a gene and to express an ectopic copy of a variant protein. The RNAi construct uses a procyclin promoter (grey rectangle) to drive transcription from two tetracycline operator sequences (lavender rectangles) to deplete the gene (blue object). The variant mRNA is produced from an overexpression construct containing a T7 promoter (brown region), one tetracycline operator and a recoded (red region) copy of the PTP (yellow rectangle) tagged gene used to avoid target by RNAi. Both plasmids get integrated into the rDNA spacer region of the cells.

MATERIALS AND METHODS

Construction of the POLIB variants.

The protein coding sequence of *TbPOLIB* (Tb927.11.4690) was PCR amplified from *T.brucei* 427 gDNA using primers MK776 and MK777 and ligated into XhoI and XbaI sites of the pLEW100-PTP-Puro (Miller et al., 2020) to generate pLEW100-FLPOLIB-PTP. The plasmid was then digested with XhoI and BamHI to remove the region to be replaced by the recoded *POLIB* sequence. The first 1053 bp of *POLIB* was synthesized by Genescript (pUC57) that included a recoded region (274 – 804 bp) by incorporating at least one silent mutation every 12 bp to make a version of *POLIB* that is RNAi resistant using reported *T. brucei* codon optimization (Horn, 2008). The 1053 bp *POLIB* region was amplified from pUC57 with primers UM55 and UM56 to add sequence homologous to pLEW100-FLPOLIB-PTP for Gibson assembly (Takara In-Fusion Kit) following manufacturer's instructions to form the resulting plasmid pLEWIBrecWT-PTP. To create the POLIB polymerase domain mutant, Asp-to-Ala mutations (D1117A, D1309A) were introduced into pLEWIBrecWT-PTP using mutagenic primers UM108 and UM109 in the same reaction with the QuikChange Lightning Multi-Site Mutagenesis Kit (Agilent) according to manufacturer's protocol. All DNA constructs and point mutations were verified by direct sequencing. All primers are listed in Table 1 in Appendix A.

Trypanosome cell culture and transfection.

Trypanosoma brucei procyclic 29-13 cells (Wirtz et al., 1999) were cultured at 27˚C in SDM-79 medium supplemented with 15% heat inactivated fetal bovine serum, 15 μg/ml G418 and 50 μg/ml hygromycin (GH). Parental RNAi cell line SLIB 2C7 was generated as previously described and grown in GH medium supplemented with 2.5 μg/ml phleomycin (GHP) (Bruhn et al., 2010). The *POLIB* variant constructs (15 μg) were linearized with Not I and transfected by nucleofection using the Amaxa Nucleofection Parasite Kit (Lonza) into procyclic *T. brucei* 29-13 cells to generate inducible overexpression POLIB variant cell lines (OE) and into SLIB 2C7 RNAi cell line (Bruhn et al., 2010) to

generate complementation cell lines (RNAi + OE). Following selection with 1.0 μg/ml puromycin, cell lines were cloned by limiting dilution as previously described (Chandler et al., 2008). All cell lines were maintained at a concentration between 5 x 10^5 – 1 x 10^7 cells/ml and continuously passaged for not more than three weeks. Cell density was determined using a Beckman Coulter Z2 particle counter. To minimize variation in data processing, all samples were collected on the same day using staggered inductions. Cell lines were induced by adding 4 μg/ml tetracycline to the growth medium unless otherwise indicated. Cultures were supplemented with 2 μg/ml tetracycline on non-dilution days to maintain RNAi and/or the expression of *POLIB* variants (Rusconi et al., 2005).

SDS-PAGE and Western Blot Analyses.

Cells were harvested for 12 minutes at 5250 x g (4°C) and washed with 1X PBS (1.37 M NaCl, 27 mM KCl, 100 mM Na_2HPO_4, 18mM KH_2PO_4) supplemented with EDTA-free protease inhibitor cocktail (Roche Diagnostics). Samples were lysed in 2X SDS sample buffer containing 5% β-mercaptoethanol. Proteins were separated by SDS-polyacrylamide gel electrophoresis and transferred to polyvinylidene membrane (PVDF) overnight at 90 mA in transfer buffer containing 10% methanol. Membranes were incubated in blocking reagent (5% non-fat dry milk) for at least one hour at room temperature followed by incubation with appropriate antibodies. PTP-tagged protein was detected with Peroxidase-Anti-Peroxidase soluble complex (PAP, 1:2000, Sigma), which recognizes the protein A domain of the PTP tag. Incubation with EF1α1 for 1 hour (1:15,000, abcam) followed by secondary HRP conjugated rabbit-anti mouse for 1 hour (1:5000, ZyMAX) was used as a loading control. Signals were detected using Clarity ECL blotting substrate (Bio-Rad) on a ChemiDoc™ Touch Imaging System. Band intensities were quantified using ImageJ software (http://imagej.nih.gov/ij/).

DNA Isolation and Southern Blot Analyses.

Total DNA was isolated from 1 x 10^8 cells using Puregene Core Kit A (Qiagen) and fractionated on a 1.5% agarose gel containing 1 μg/ml ethidium bromide for 16.5 hours at 2.4 V/cm with recirculating

1X Tris-Acetate-EDTA running buffer. Fractionated DNA was processed using standard depurination, denaturation and neutralization treatments, then transferred to GeneScreen Plus membrane using capillary transfer. The membrane was then UV cross-linked using Stratalinker UV Crosslinker (Stratagene). Membranes were probed with minicircle, and α-tubulin specific random primed radiolabelled probes as previously described (Chandler et al., 2008). Visualization and quantification were performed using a Typhoon 9210 Phosphoimager (Molecular Dynamics) with background subtraction and normalized against tubulin using ImageQuant 5.2 software.

RNA Isolation, Northern Blot and RT-qPCR.

Total RNA was isolated from 5 x 10^7 cells with Trizol and cleaned using RNA Clean and Concentrator kit (Zymo Research) according to manufacturer's instructions. RNA was separated on a 1.5% agarose/formaldehyde gel and transferred to GeneScreen Plus membrane (Perkin Elmer). The specific mRNAs were detected with ^{32}P random prime-labeled probes, and the signals were quantified as previously described (Chandler et al., 2008). RNA concentrations were determined using nanodrop spectrophotometer (Thermo Fisher Scientific). 100 ng of total RNA was reverse transcribed to cDNA with random primers using the High Capacity Reverse Transcription Kit (Applied Biosystems). qPCR was performed using QuantiNova SYBR Green PCR (Qiagen) with 2 µg of cDNA and 10 µM of gene specific primers per reaction (Table 1).

Immunofluorescence Microscopy.

Cells were harvested for 8 minutes at 1000 x g and resuspended in 1X PBS. Cell were then adhered to poly-L-lysine coated slides and fixed for 5 minutes in 3% paraformaldehyde. They were then washed twice in 1X PBS/0.1 M glycine, permeabilized for 5 minutes with 0.1% Triton X-100 and washed thrice with 1X PBS. PTP-tagged protein was detected with rabbit polyclonal anti-protein A (1:1000, 1hour, Sigma) and basal bodies detected with rat monoclonal antibody YL1/2 (1:3500, 1hour, Abcam) in 1X PBS containing 1% BSA. Cells were then washed thrice with 1X PBS containing 0.1% Tween-20 and incubated

with the corresponding secondary antibodies for 1 hour: Alexa Fluor 488 goat anti-rabbit (1:250) and Alexa Fluor 594 goat anti-rat (1:250) in 1X PBS containing 1% BSA. DNA was stained with 7 ug/ml of 4′,6-diamidino-2-phenylindole (DAPI) for 10 minutes, washed thrice in 1X PBS and then finally mounted in Vectashield (Vector Laboratories). Cells were analyzed using a Nikon Eclipse E600 microscope and the images were captured and processed using the SPOT software 5.2. Changes in the morphology of kDNA network were quantified as described previously (Bruhn et al., 2010; Chandler et al., 2008) with a minor modification. In addition to scoring karyotype of the nucleus and kDNA, the number of basal bodies was used to determine the cell cycle stage especially related to replicating kDNA where 2 basal bodies indicates that the kDNA is undergoing replication (1N1K2BB) or has already segregated into 2 separate networks (1N2K2BB).

RESULTS

Screening of overexpression clones

Similar to other replicative proofreading DNA polymerases, POLIB contains polymerase and exonuclease domains each with the conserved active site residues. Previously, *TbPOLIB* was silenced using an intramolecular stemloop double stranded RNA trigger which led to a reduced growth rate, progressive loss of the kDNA network, and disruption of minicircle replication indicating that *POLIB* had an essential role in kDNA replication (Bruhn et al., 2010). It was assumed that nucleotidyl incorporation would be essential for the role in kDNA replication. However, it is possible that the polymerase domain may not be essential for the function of POLIB. In budding yeast, the DNA polymerase and proofreading exonuclease activity of DNA polymerase epsilon are not essential for cell growth, whereas the non-catalytic C-terminal domain of the protein is required (Dua et al., 1999, Kesti et al., 1999). To evaluate whether the polymerase domain is necessary for the essential replicative role of POLIB, an RNAi-complementation system was designed to study the functions of the two distinct POLIB domains. This study will focus on establishing the complementation system and evaluating the role of the polymerase domain.

Targeting the 3'UTR of a gene and co-expression of an ectopic copy of the RNAi target is a validated approach for *in vivo* complementation in *T. brucei* (Kaser et al, 2016, Ralston et al., 2011, Trikin et al., 2016, Weems et al., 2015, Yu et al., 2012). However, the extremely short 3' UTR (none reported) and 5' UTR (89 bp) of *TbPOLIB* are not recommended for RNAi (UTR sequences obtained from https://tritrypdb.org). To circumvent this, the portion of the *TbPOLIB* gene that was previously targeted by RNAi was recoded to generate an RNAi resistant version of POLIB. Transfection of 29-13 cells with pLewIB-WTPTP^{Puro} containing the recoded and C-terminally PTP-tagged version of POLIB (see methods) was used to study the effects of increased POLIB protein in the absence of RNAi. The resulting inducible overexpression (OE) cell line IBWT^{PTP}

was subjected to dilution cloning. Eleven clonal cell lines were induced with 1 μg/ml tetracycline for 2 days to evaluate protein expression, and impact on fitness. Western blot analysis revealed that all but one of the clones expressed the recoded IBWT^{PTP} variant at levels that exceeded those of endogenous POLIB levels from a cell line engineered to express epitope-tagged POLIB from a single allele (+C) (Appendix B1, A). Clone P1D12 was selected for further characterization based on a doubling time of 13.2 hours and consistent protein expression (5.7 fold) above endogenous POLIB-PTP levels. Doubling time for the parental 29-13 cell line was 12.9 hours.

To study whether the polymerase domain is essential for function, a recoded variant that has the two active site Asp residues mutated to Ala (D1117A, D1309A) was generated while leaving the exonuclease active site residues intact. Transfection of 29-13 cells with pLewIB-Pol-PTP^{Puro} was used to study the effects of increased POLIB mutant protein in the absence of RNAi. The resulting inducible overexpression (OE) cell line IBPol-^{PTP} was subjected to dilution cloning. Eight clonal cell lines were induced with 1 μg/ml tetracycline for 2 days to evaluate protein expression, and impact on fitness. Western blot analysis revealed that all the clones expressed the recoded IBPol-^{PTP} variant. (Appendix B1, B). Clone P1D8 was selected based on the doubling time of 14.65 hours and consistent protein expression levels (8.5 fold) above POLIB-PTP levels for further characterization.

Characterization of IBWT^{PTP} OE clone P1D12

Overexpression of recoded IBWT^{PTP} variant (clone P1D12) in the absence of POLIB RNAi was evaluated for an extended period of time to determine whether POLIB overexpression had an impact on cells. An 8 day induction with 1 μg/ml tetracycline resulted in no significant change in growth rate (Figure 5A). Western blot analyses revealed a 11.6 fold increase in protein levels compared to endogenous POLIB with minimal proteolytic degradation (Figure 5B). By analyzing the free minicircle population using Southern blotting and a minicircles specific probe, both unreplicated CC monomers and newly replicated N/G molecules remained unchanged when this variant was

overexpressed (data not shown). Lastly, fluorescence microscopy revealed that a great majority of the cells equally expressed the IBWT^{PTP} throughout the mitochondrion (Figure 5C). These data indicate that extended overexpression of IBWT^{PTP} had no detectable impact on cell fitness.

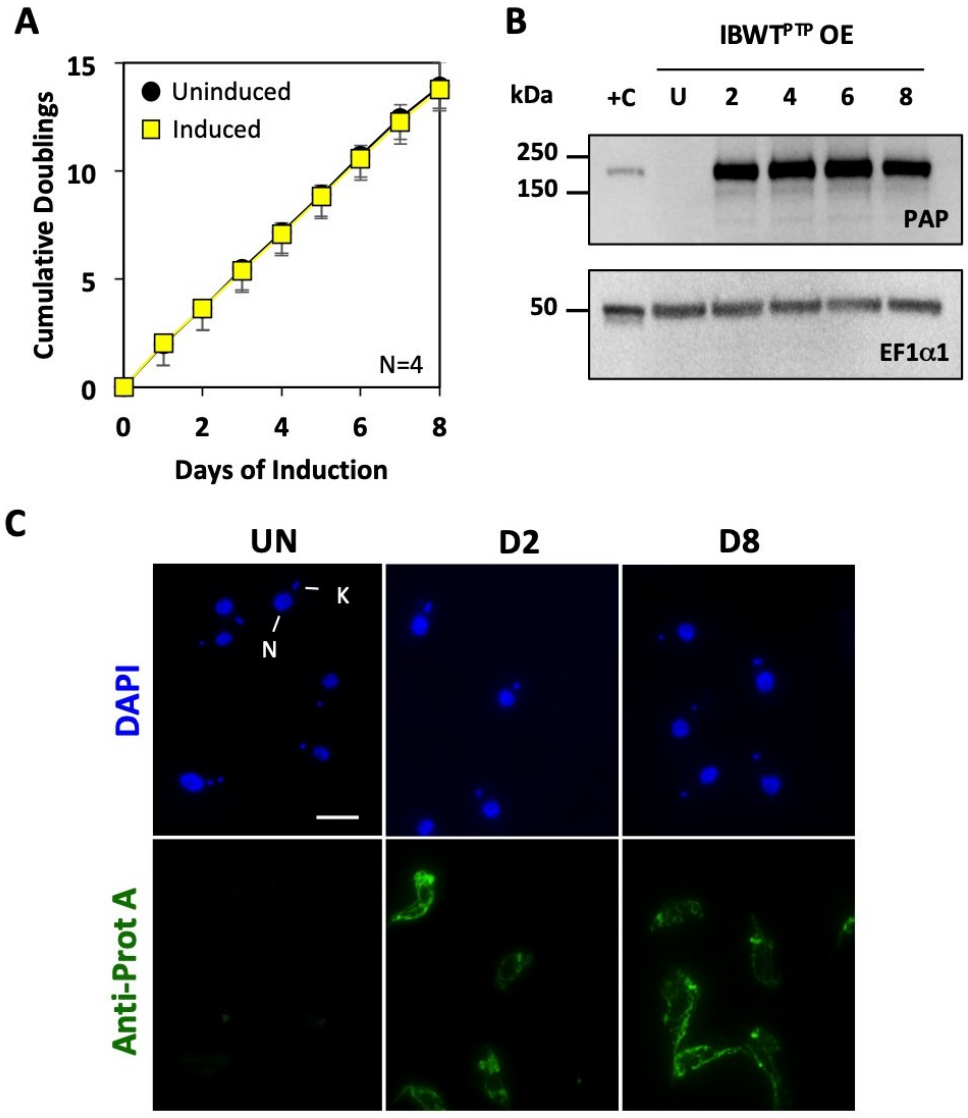

Figure 5: Overexpression of IBWT^{PTP} in procyclic cells.

A) Clonal cell line IBWT^{PTP} OE P1D12 was grown in the absence and presence of 1 µg/ml tetracycline. Error bars represent the ±s.d. of the mean from four biological replicates. B) Representative Western blot detection of IBWT^{PTP} and loading control EF1α1 during an 8 day induction. 2 x 10^6 cell equivalents were loaded into each well. +C, single allele control cell line endogenously expressing POLIB-PTP. C) IBWT^{PTP} OE P1D12 cells were stained/labeled with DAPI (blue) and anti-protein A (green). Representative images showing expression of IBWT^{PTP} at selected time points. N, Nucleus; K, kDNA. Size bar, 5 µm.

Characterization of IBPol-^{PTP} OE clone P1D8

Similar to the IBWT^{PTP} variant, the effects of overexpressing the POLIB polymerase domain mutant for 8 days were studied. Overexpression of the recoded IBPol-^{PTP} variant (clone P1D8) in the absence of *POLIB* RNAi resulted in a negligible change in growth rate at day 6 (Figure 6A). This small reduction in fitness was consistent among the four different inductions that were performed. Western blot analyses showed that there was a 9.6 fold increase in protein expression levels above POLIBWT^{PTP} levels that were maintained across the 8 day induction (Figure 6B). Fluorescence microscopy revealed homogeneous expression of IBPol-^{PTP} within the cell population (Appendix B3, A). To determine if the small reduction in fitness impacted kDNA replication, Southern blot analyses were performed to detect any subtle changes in the free minicircle replication intermediates. Similar to the IBWT^{PTP} variant, there was no significant change in the free minicircle populations (Figure 6C). These data indicate that extended overexpression of IBPol-^{PTP} had no measurable impact on kDNA replication.

Establishing the POLIB dually inducible RNAi complementation system

POLIB plays an essential role at the core of the minicircle replication machinery. To examine the importance of the individual POLIB domains, an RNAi complementation was established (Figure 4). To determine if the deficiencies caused by *POLIB* RNAi could be rescued by ectopic expression of PTP tagged wild-type POLIB (IBWT^{PTP}), the parental RNAi cell line SLIB 2C7 was transfected with pLewIBWT-PTP^{Puro}. Following selection of a stable population with puromycin, the complementation cell line (IBRNAi + IBWT^{PTP}) was subjected to dilution cloning. Ten clonal cell lines were induced with 1 μg/ml tetracycline for 2 days to evaluate protein expression. Western blot analyses revealed that all the clones expressed the recoded IBWT^{PTP} variant at 0.4 fold levels below endogenous single expressor POLIBWT^{PTP} protein levels (Figure 7), while knockdown of *POLIB* mRNA was approx. 80-90%, consistent with previously published data (Bruhn et al., 2010). Increasing tetracycline

concentration could be used to achieve higher protein expression levels. Previously, all data from silencing POLIB was acquired using the lower 1 μg/ml tetracycline concentration. It was vital to establish that using a higher tetracycline concentration would have no impact on the 29-13 cells and would not saturate the RNAi machinery.

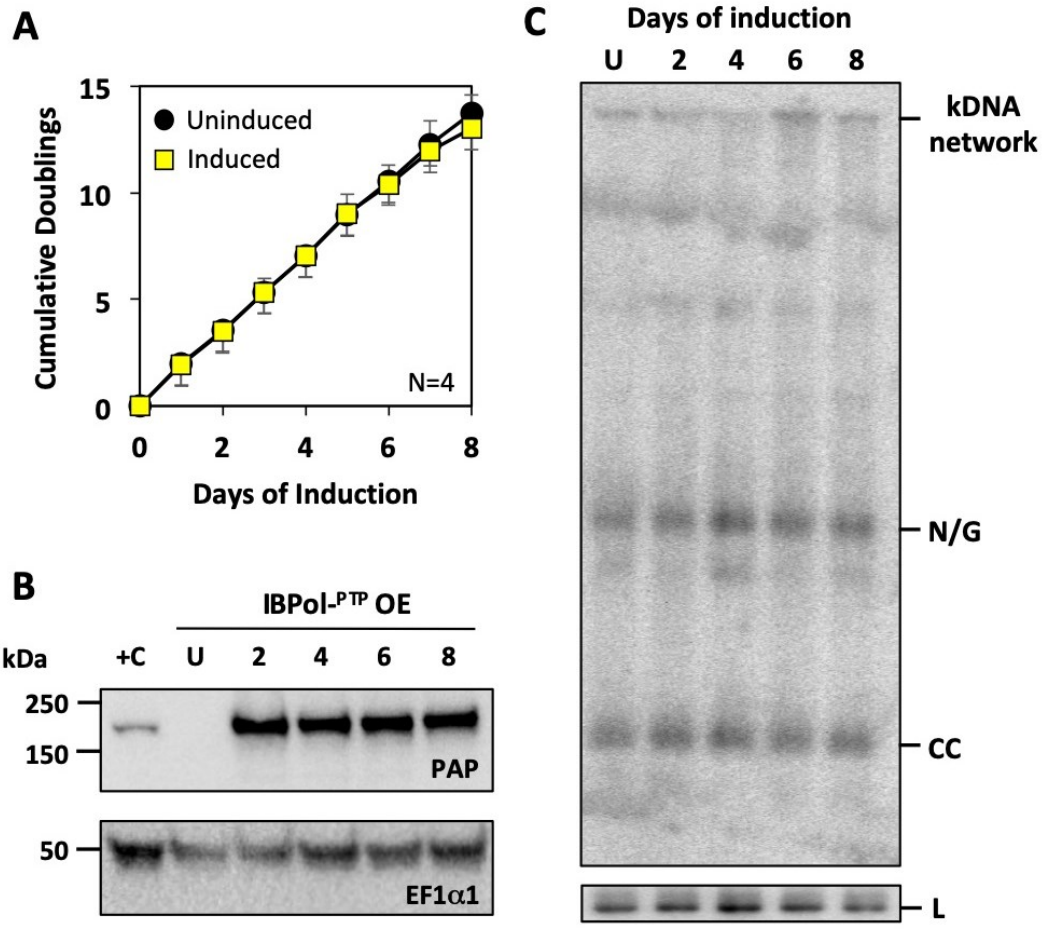

Figure 6: Overexpression of IBPol-^{PTP} in procyclic cells.

A) Clonal cell line IBPol-^{PTP} OE P1D8 was grown in the absence and presence of 1 μg/ml tetracycline. Error bars represent the ±s.d. of the mean from four biological replicates. B) Western blot detection of the PTP tag and loading control EF1α1 during an 8 day induction. 2 x 10^6 cell equivalents were loaded into each well. +C, single allele control cell line endogenously expressing POLIB-PTP. C) Representative Southern blot showing no change in the free minicircle population. k, kDNA network; N/G, nicked/gapped; CC, covalently closed; L, loading control. Data are normalized to the tubulin loading control.

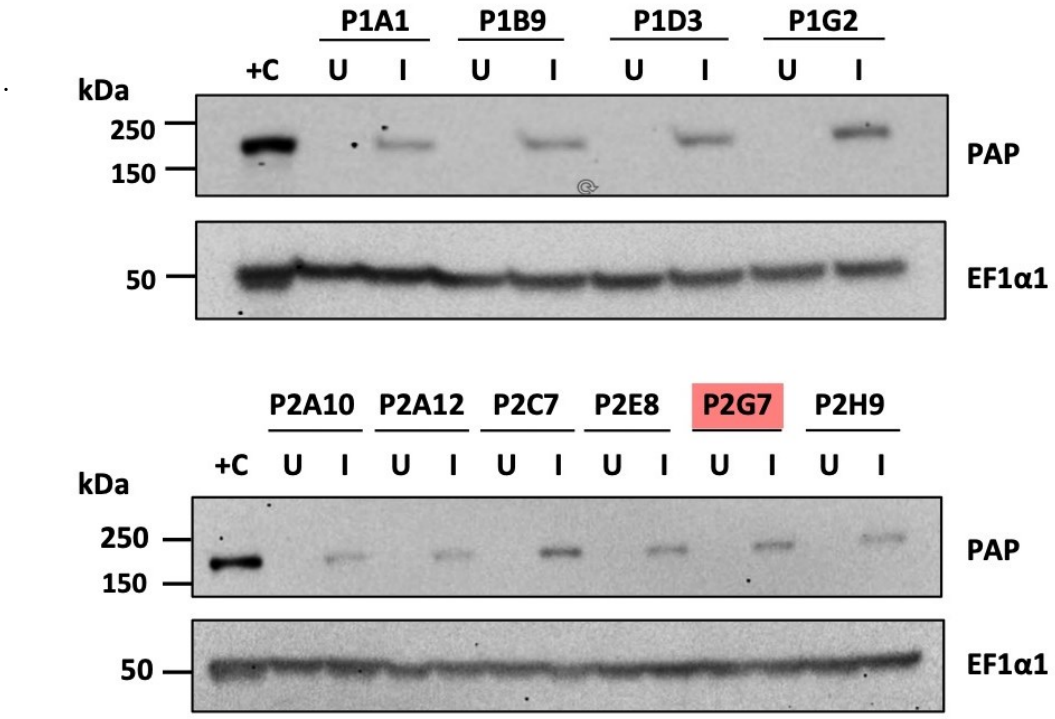

Figure 7: Dual Induction of *POLIB* RNAi and IBWT^{PTP} variant.
Clonal cell lines were induced with 1 µg/ml tetracycline for 2 days to screen for protein expression. Western blot detection of IBWT^{PTP} variant and EF1α1 from whole cell lysates. Screen of 10 IBRNAi + IBWT^{PTP} clones. +C, single allele control cell line endogenously expressing POLIB-PTP; U, Uninduced; I, Induced. 2 x 10^6 cell equivalents were loaded into each well. Clone labeled with red box were selected for further characterization.

The procyclic 29-13 cell line harbors T7 RNA polymerase and TET repressor and is commonly used for many inducible expression studies (Wirtz et al., 1999). When these cells are grown in the absence or presence of 1 µg/ml, 2 µg/ml and 4 µg/ml tetracycline, there was no change in fitness (Figure 8A). Inducing POLIB RNAi at the three differing concentrations of tetracycline produced similar loss of fitness that closely resembled the previously reported data. RT-qPCR analyses revealed 80.9%, 86.8% and 99.8% knockdown of endogenous *POLIB* mRNA levels at 1 µg/ml, 2 µg/ml, and 4 µg/ml of tetracycline respectively, indicating that increasing amounts of tetracycline improved the knockdown of *POLIB* and did not saturate the RNAi machinery (Figure 8B). To detect subtle changes in the free minicircle population that might occur at the differing tetracycline concentrations, Southern blotting with a minicircle specific probe indicated similar patterns for both unreplicated CC monomers and newly replicated N/G molecules across the three separate tetracycline inductions (Figure 8C).

Subsequent experiments used 4 μg/ml of tetracycline inducer to obtain higher levels of ectopically expressed POLIB variant during complementation experiments.

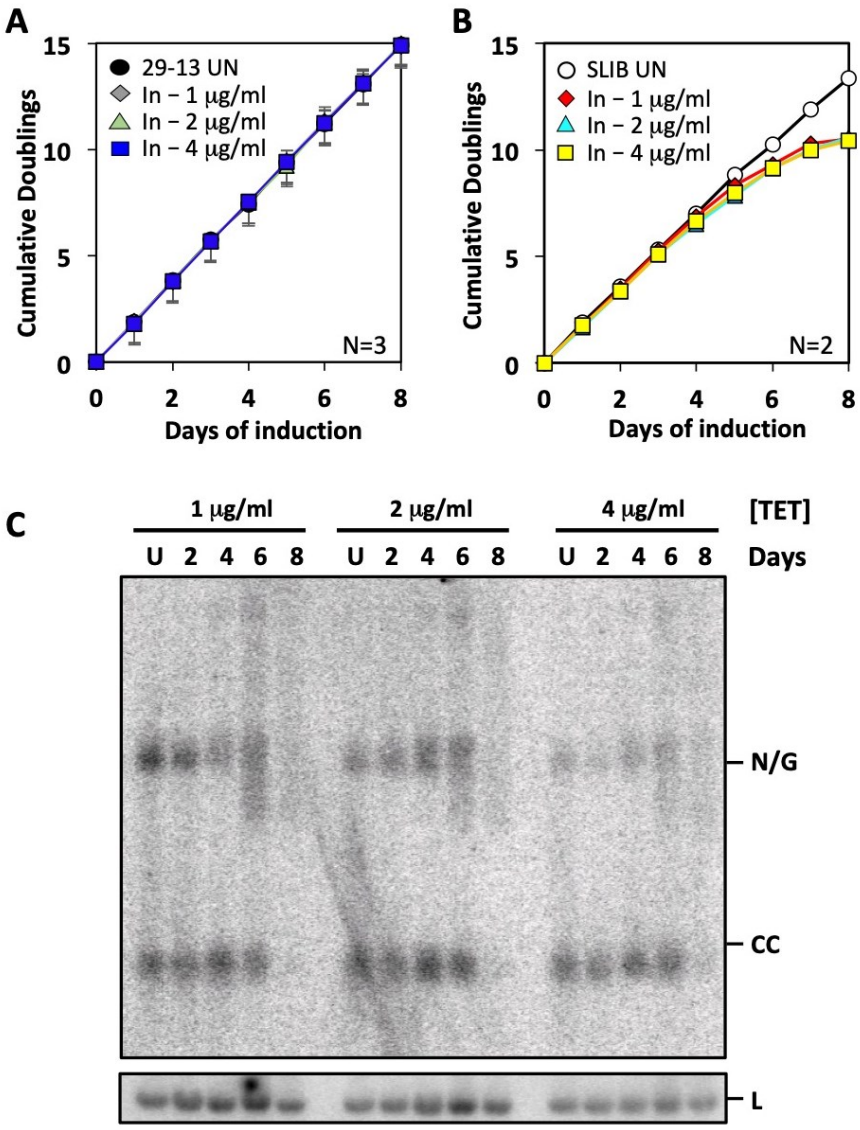

Figure 8: Effects of increasing concentrations of tetracycline on trypanosome growth.
A) 29-13 procyclic cells were grown in the absence and presence of increasing concentrations of tetracycline. Values are the mean (± standard deviation) from three independent replicates. **B)** Clonal cell line SLIB 2C7 was grown in the absence and presence of increasing concentrations of tetracycline to express *POLIB* stem-loop dsRNA. Values are the mean from two independent replicates. **C)** Representative Southern blot showing the decrease in free minicircle species during *POLIB* silencing at three concentrations of tetracycline. N/G, nicked/gapped; CC, covalently closed; L, loading control. Data are normalized to the tubulin loading control.

Two IBRNAi + IBWT^{PTP} clones (P1B9, P2G7) were selected based on a doubling time of 13.85 hours and IBWT^{PTP} protein levels (0.3 fold) and grown in absence and presence of 4 µg/ml tetracycline to evaluate whether IBWT^{PTP} could rescue the POLIB RNAi phenotype. Clones P1B9 and P2G7 showed similar growth kinetics and displayed better fitness than the parental SLIB RNAi cell line indicating a partial rescue (Figure 9A). Northern blot analyses following 48 hours of induction revealed robust knockdown for *POLIB* mRNA when the two clones were induced with the higher concentrations of tetracycline: P2G7, 93% and P1B9, 89.9% 98.5% for 2 and 4 µg/ml respectively (Figure 9B).

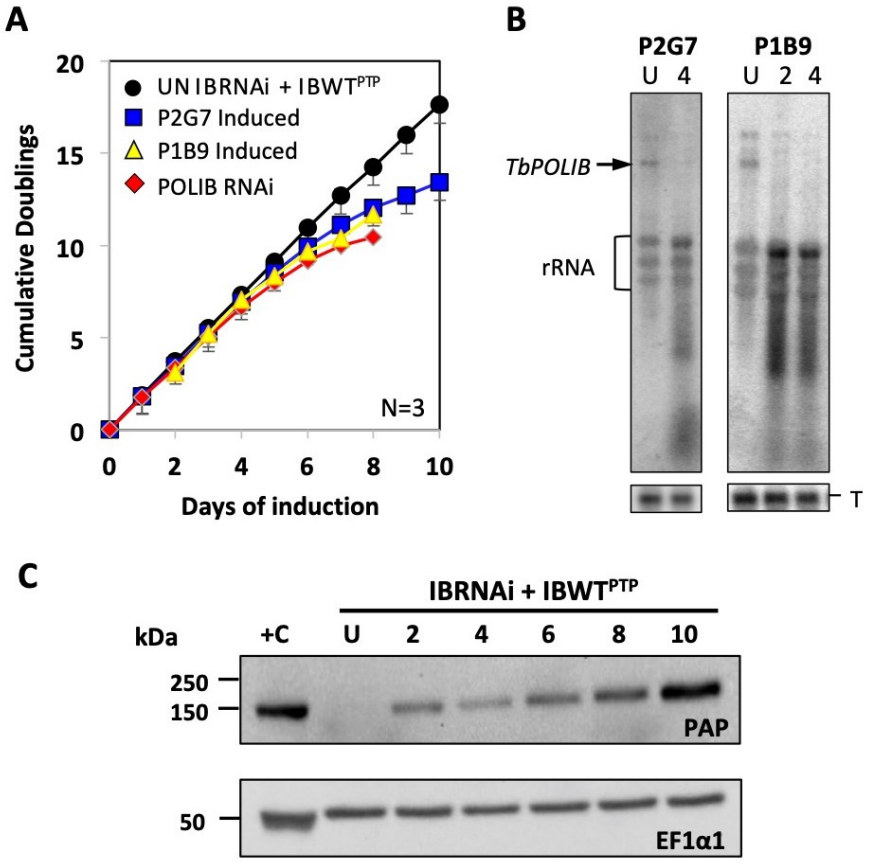

Figure 9: Incomplete rescue of POLIB RNAi with ectopically expressed IBWT^{PTP}. A) Growth curve of uninduced, tetracycline-induced IBRNAi + IBWT^{PTP} clones and parental POLIB RNAi procyclic cells. Values are the mean (± standard deviation) from three independent replicates for clone P2G7. **B)** Northern blots of total RNA from uninduced (U) and cultures induced with 2 µg/ml (2) or 4 µg/ml tetracycline (4) for 48 hours hybridized with radiolabeled probe specific for POLIB. Hybridization with α-tubulin was the loading control. **C)** Representative Western blot of IBWT^{PTP} and EF1α1 levels over 10 days of induced complementation for clonal cell line P2G7.

Western blot data revealed a gradual increase in the levels of IBWT^{PTP} over the induction period with the highest levels (2.3 fold above endogenous levels) of the variant detected at Day 10 (Figure 9C). The delay in attaining sufficient protein levels higher than endogenous single expressor POLIBWT^{PTP} could have something to do with the lack of a complete rescue of the POLIB silencing phenotype. Lastly, fluorescence microscopy indicated that a majority of the cells displayed low levels of IBWT^{PTP} protein while only a minor subset of the population displayed a robust fluorescent signal (Appendix B2, B). This is in striking contrast to cells overexpressing IBWT^{PTP} alone.

To assess the effects on kDNA network morphology, uninduced and induced IBRNAi + IBWT^{PTP} cells were DAPI-stained and examined by fluorescence microscopy to manually score the size of the kDNA network (150 cells per data point) and karyotype on the duplication and segregation of the nuclear (N), kDNA (K), and basal bodies. Uninduced cells exhibited normal duplication and segregation of the nuclear (N) and kDNA (K) genomes with each cell cycle karyotype easily observed [1N1K, 1N1K* (replicating kDNA), 1N*2K (replicating nucleus) and 2N2K] (Figure 10A). In contrast, induced cells exhibited progressive shrinking and loss of the kDNA network (Figure 10A and B).

A significant proportion of the cells displayed kDNA morphological defects by Day 6 with the accumulation of cells containing small kDNA and no kDNA (dyskinetoplastic)(Figure 10B). By Day 8, only 15% of the cell population still contained normal-sized kDNA, while the remaining population contained small kDNA (58%) or no kDNA (mean 25%). While complementation with IBWT^{PTP} led to the progressive loss of kDNA, it resulted in the majority of cells displaying a small kDNA phenotype rather than complete loss of kDNA as previously reported for the POLIB RNAi phenotype (Bruhn et al., 2010).

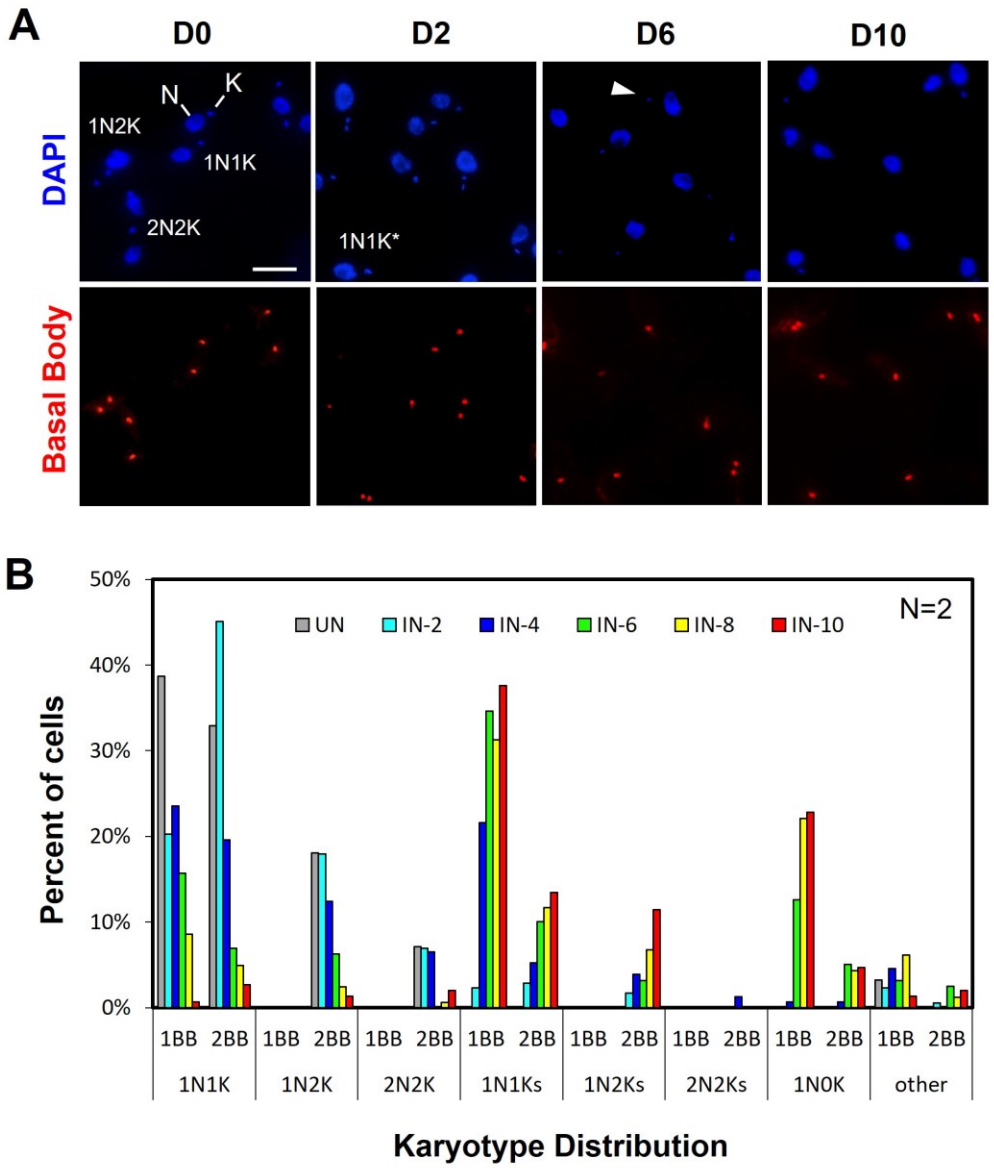

Figure 10: Effects of IBRNAi + IBWT^{PTP} on kDNA morphology.
Clonal cell line IBRNAi + IBWT^{PTP} P2G7 was grown in the absence and presence of 4 µg/ml tetracycline. **A)** Top panel, DAPI-stained fluorescent images; Bottom panel, YL1/2 stained basal bodies. Representative images for the indicated time points showing kDNA morphology. N, nucleus, K, normal sized kDNA; * replicating kDNA; arrowhead, small kDNA; arrow no kDNA. Scale bar, 5 µm. **B)** Quantification of kDNA morphology. DAPI and YL1/2 stained cells were scored for number of nuclei, kDNA and basal bodies. 150 cells were randomly selected and scored for each time point. Values are the mean of two separate inductions.

Silencing of *POLIB* led to disruption of minicircle replication intermediates with the accumulation of a novel population of covalently closed minicircle dimers (fraction U) and unreplicated covalently closed precursors as the most abundant free minicircle species during loss of the kDNA network

(Bruhn et al., 2010). To study the changes in kDNA at a molecular level, Southern blot analyses were performed to detect changes in the free minicircle replication intermediates during IBWT^{PTP} complementation. In uninduced cells, CC monomers (replication precursors) and newly replicated nicked/gapped (N/G) progeny are present at a 4:1 ratio. The relative concentration of free minicircles changed minimally during the induction. The total abundance of free minicircles declined and Fraction U started to accumulate but was not the major free minicircle species. Together these data indicate that complementation with IBWT^{PTP} can partially rescue the loss of fitness, loss of kDNA, and disruption to minicircle replication intermediates when POLIB is silenced.

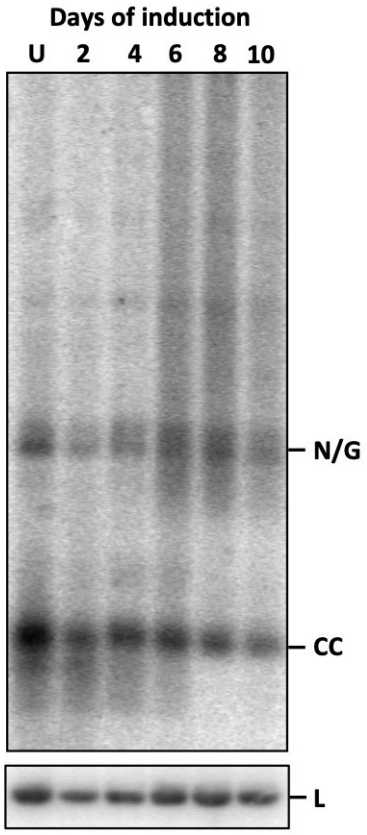

Figure 11: Changes in the free minicircle population during IBRNAi + IB-WT OE.
Clonal cell line IBRNAi + IBWT^{PTP} P2G7 was grown in the absence and presence of 4 μg/ml tetracycline. **A)** Southern blot detected with a radiolabeled probe. N/G, nicked/gapped; CC, covalently closed; L, loading control. Data are normalized to tubulin.

Expression of IBPol-PTP variant does not rescue POLIB RNAi

To determine the effect of ectopic expression IBPol-^{PTP} in the presence of POLIB RNAi, the parental RNAi cell line SLIB 2C7 was transfected with pLewIBPoldeadPTP^{Puro} and subjected to dilution cloning. Ten clonal cell lines were induced with 1 μg/ml tetracycline for 2 days to evaluate protein expression. Western blot analyses revealed that all the clones expressed IBPol-^{PTP} 0.2 fold below endogenous POLIB levels (Appendix B3). Two IBRNAi + IBPol-^{PTP} clones (P2C9, P2F9) were selected and grown in the presence of 4 μg/ml tetracycline. Both clones displayed similar growth kinetics and displayed the same loss of fitness as the original *POLIB* RNAi cell line (Figure 12A). Following 48 hours of induction, Northern blot analyses revealed an 87.3% and 89.4 % reduction of endogenous *POLIB* mRNA transcript for clones P2C9 and P2F9, respectively (Figure 12B). Western blot data revealed consistent but moderate levels of IBPol-^{PTP} variant over the induction period (Figure 12C). Fluorescence microscopy indicated that a majority of the cells displayed low levels of IBPol-^{PTP} protein while only a minor subset of the population displayed a robust fluorescent signal (Appendix B4, B). Lastly, Southern blot analyses of free minicircle species revealed few changes in the proportion of CC and N/G free minicircles over the course of the induction. However, the accumulation of Fraction U was most evident at Day 8, similar to POLIB RNAi alone.

IBPol-^{PTP} complementation also resulted in a progressive loss of kDNA (Figure 13A, B). However, the kinetics differed significantly from IBWT^{PTP} complementation or POLIB RNAi alone. The accumulation of cells with small kDNA networks was evident as early as Day 2 already representing 28% of the population. By Day 4, cells with small kDNA represented the great majority of the population (93%), and continued as the predominant cell type throughout the induction (74%). By day 8, approximately 20% of the cells lacked kDNA. This data indicate that the POLIB polymerase domain contributes to maintenance of the kDNA network.

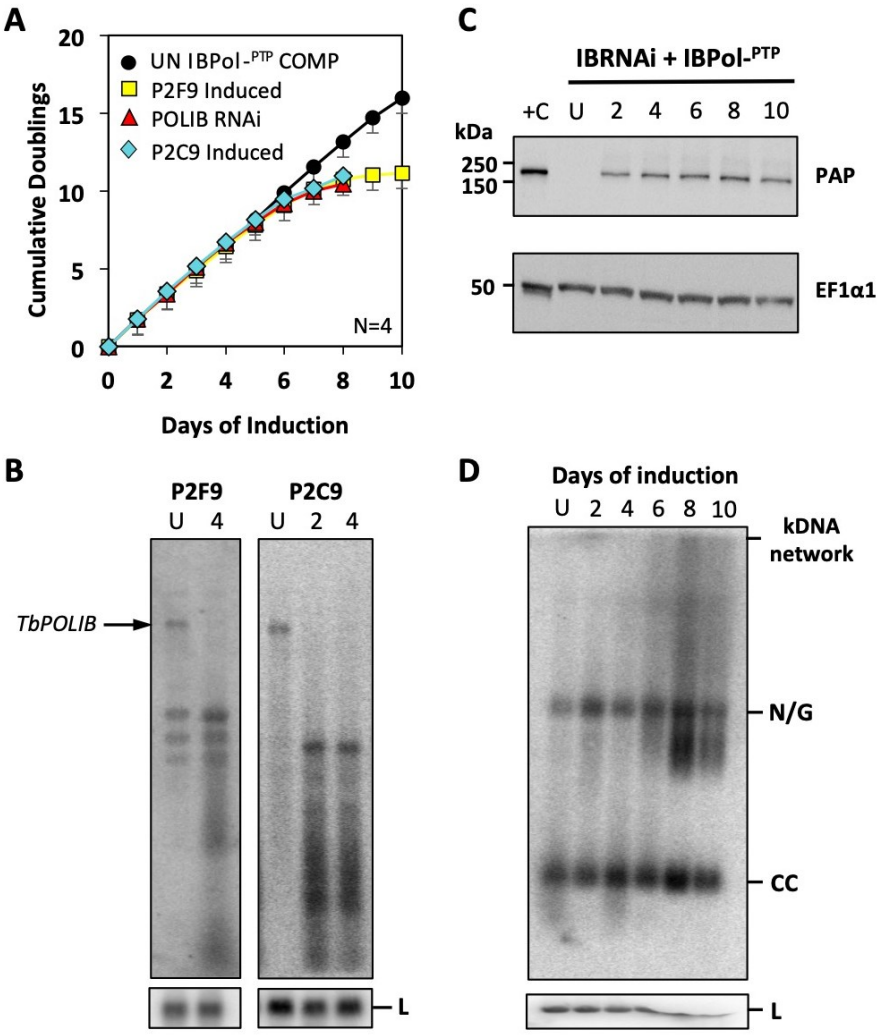

Figure 12: Expression of IBPol-^{PTP} does not rescue *POLIB* RNAi

A) Growth curve of uninduced, tetracycline-induced IBRNAi + IBPol-^{PTP} clones and parental *POLIB* RNAi procyclic cells. Values are the mean (± standard deviation) from three independent replicates for clone P2F9. **B)** Northern blots of total RNA from uninduced (U) and cultures induced with 2 µg/ml (2) or 4 µg/ml tetracycline (4) for 48 hours hybridized with radiolabeled probe specific for POLIB. Hybridization with a-tubulin was the loading control. **C)** Representative Western blot detection of IBWT^{PTP} and EF1a1 levels over 10 days of induced complementation for clonal cell line P2F9. **D)** Southern blot showing changes in the free minicircle population detected with radiolabeled minicircle probe. N/G, nicked/gapped; CC, covalently closed; L, α-tubulin loading control.

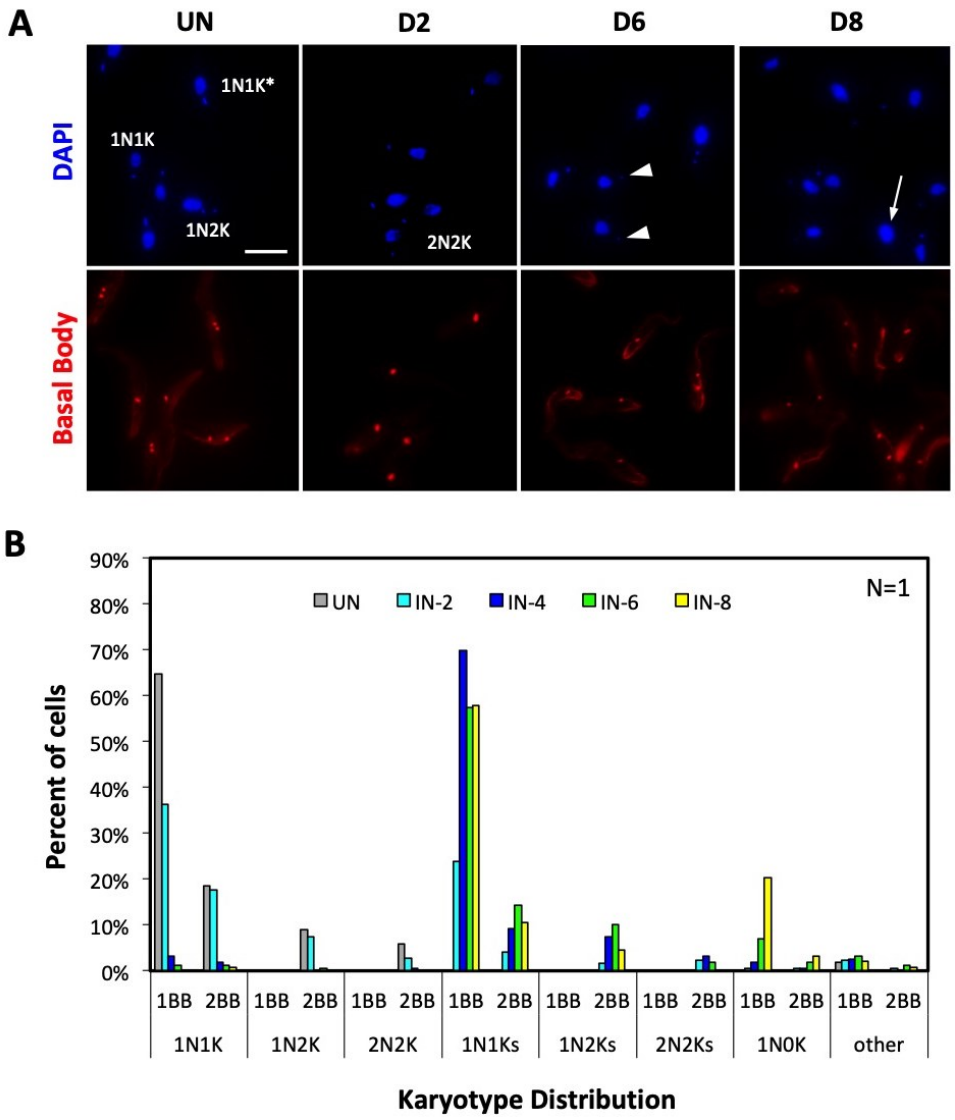

Figure 13: Effects of IBRNAi + IBPol-^{PTP} on kDNA morphology.
Clonal cell line IBRNAi + IBPol-^{PTP} P2F9 was grown in the absence and presence of 4 µg/ml tetracycline. **A)** Top panel, DAPI-stained fluorescent images; Bottom panel, YL1/2 stained basal bodies. Representative images for the indicated time points showing kDNA morphology. N, nucleus, K, normal sized kDNA; *replicating kDNA; arrowhead, small kDNA; arrow no kDNA. Scale bar, 5 µm. **B)** Quantification of kDNA morphology. DAPI and YL1/2 stained cells were scored for number of nuclei, kDNA and basal bodies. 150 cells were randomly selected and scored for each time point.

DISCUSSION

Mitochondrial DNA replication in trypanosomes is a complex process that involves a multiplicity of DNA polymerases that play non-redundant roles in the overall maintenance of the network. Amongst the Family A mitochondrial DNA polymerases in trypanosomes, POLIB, IC and ID are essential for growth and kDNA maintenance. The presence of 4 independent Pol I-like mitochondrial DNA polymerases in kinetoplastids is unprecedented among eukaryotes (Figure 1). One feature of POLIB not found in any other family A DNA polymerase is the presence of an exonuclease domain embedded within the polymerase domain (Figure 3).

Interestingly, the 4 mitochondrial DNA polymerases and the unique POLIB domain structure is conserved among all kinetoplastid organisms sequenced thus far (Figure 1A) (TritrypDB.org).

The exact contributions of the annotated domains to the essential function of POLIB are unclear. While CRISPR tools have recently been developed for the closely related trypanosomatid *T. cruzi* and *Leishmania*, they have not been optimized for use in *T. brucei*. Therefore, RNAi is still the best genetic tool for studying the function of a gene in African trypanosomes.

In this body of work, we established a dually inducible RNAi plus overexpression complementation system to study the roles of the two predicted domains in the overall function of POLIB *in vivo*. We predicted that the predominant role of POLIB was nucleotidyl incorporation that resides in the DNA polymerase domain. To test our hypothesis, we investigated the structure-function relationship by ectopically expressing POLIB variants in *T. brucei* depleted of endogenous POLIB. To establish the complementation system, the PTP tagged variant proteins were first expressed in the cells using standard levels of tetracycline. The variant protein levels were abundant and well above POLIBWT^{PTP} levels. Microscopy indicated homogeneous expression of the variant protein in most cells. The high levels of the variant protein being produced neither caused a growth defect nor impaired the kDNA replication machinery as observed by growth curve, Southern blot analyses and microscopy. This was conclusive that the variants intrinsically did not have any negative effects on the cells.

The complementation system as described in Figure 4 allows for simultaneous tetracycline inducible expression of a dsRNA to deplete a gene and co-express a protein within the same inducible system. Initial western blot analysis revealed that the cells were expressing the recoded wildtype variant levels 0.4 fold below endogenous POLIBWT^{PTP} protein levels. To address this, an adaptation was made to the complementation system by increasing the concentration of the tetracycline inducer to ensure maximal levels of variant protein being produced. It was necessary to be certain that using a non-standard and higher concentration of tetracycline was neither saturating the RNAi machinery of the parental *POLIB* RNAi cell line nor impacting normal cell growth in 29-13 cells. 29-13 cells grown in the absence or presence of different concentrations of tetracycline displayed no change in fitness. Inducing *POLIB* RNAi with the different concentrations of tetracycline produced a similar growth defect. RT-qPCR analyses revealed an increase in *POLIB* gene knockdown by using higher concentrations of tetracycline. Southern blot analyses indicated similar patterns for both covalently closed and nicked/gapped minicircle species.

In the complementation cell lines, induction with a higher concentration of tetracycline (4 μg/ml) resulted in higher levels of variant protein being produced, but they were still below endogenous POLIBWT^{PTP} levels. Majority of the cells displayed low levels of the variant protein while only a small subset displayed robust fluorescent signal. The RNAi vector used for the complementation system is driven by the procyclin promoter and contains two tetracycline operator sequences that must be unbound from the repressor using tetracycline. In the overexpression vector, a strong T7 promoter upstream of just one tetracycline operator sequence drives transcription. The high knockdown of the endogenous gene and low levels of variant protein being produced suggests that there is an unexplainable preference for tetracycline to bind first to the two operators in the RNAi vector. The deficiency in the variant protein being produced especially during the critical time points where the cells begin to lose fitness could be the reason why there is an incomplete rescue of the growth phenotype.

In the parental *POLIB* RNAi cells, microscopy revealed that 54% of the total population of cells had no kDNA by 10 days of RNAi and 40% of the cells had small kDNA (Bruhn et al., 2010). In the IBRNAi + IBWT^{PTP} cells, about 28% of the total population had no kDNA by 10 days of induction and 62% of the

cells had small kDNA. It is evident that complementation with the wildtype protein slowed down the accumulation of dyskinetoplastic cells. The lack of complete rescue of the *POLIB* RNAi phenotype suggests that the expression of POLIB is so tightly controlled that even a moderate change from wildtype expression levels can irreversibly impact fitness. It also could be due to insufficient protein production at the critical time points when loss of kDNA reaches a certain threshold. The RNAi vector has two operator sequences that must be unbound from repressor as opposed to the overexpression vector that has just one tetracycline operator. Despite this, it's clear from northern blot and western blot that RNAi induction is preferentially favored over expression of variant protein. The lack of precise and independent control over the expression of exogenous mutants and RNAi is critical. To address this, the vanillic acid inducible system (Sunter, 2016) adapted as SMUMA can be used to operate simultaneously with the tetracycline-based system. SMUMA (Single Marker UMAss) carries T7 RNA polymerase, tetR and vanillic acid repressor (vanR). The RNAi vector and the overexpression plasmid we used in our experiments, upon transfection into *T. brucei*, get targeted to the rDNA spacer region, a non-transcribed chromosomal locus. A potential solution would be to use another RNAi vector that gets integrated into a different chromosomal locus like the minichromosomes of trypanosomes (Wickstead et al., 2003). There are many open questions as to how the complementation system can be modified in order to attain maximal levels of protein. Southern blotting to examine specific effects on the maxicircle populations may provide further insight. At this point, it is not possible to reach a conclusion about the exact role of the polymerase domain, but this body of work suggests that the domain is likely essential for the role of POLIB in kDNA replication.

APPENDICES

Appendix A

Table A1. List of primers used in this study.

Underline, restriction enzyme sites; lowercase letter, plasmid backbone sequence

Gene	Purpose	Primer Name	Primer Sequence	Linker
TbPOLIB (927.11.4690)	**Subcloning**	MK776	5'-GTA ACT CGA GAT GCG GCT AAA TAG CTG C-3'	XhoI
		MK777	5'-ACA CTC TAG ACA CCG TAA TTT CTA CAC TGT CAG-3'	XbaI
	Gibson Assembly	UM055	5'-gct tca att gct cGA GAG ATG CGG CTA AAT AGC TGC-3'	-
		UM056	5'-gta ccg ggc cgg atc CGA CTG ATA TAC CCC ACG ATA C-3'	-
	Site directed mutagenesis	UM108	5'-GGC CGT TGC GTG GAA ATT GCC TAC TCG CAG CTG-3'	-
		UM109	5'-GAT AAA CTT CGT ACA CGC TTC GCT TTG GCT CGA C-3'	-
	qPCR	MK563	5'-GTG ATT GCA TTC ATG GCG ACG GAA-3'	-
		MK564	5'-AGT ACT TGG TCC ATG GCTCCA CAA-3'	-
TERT (927.11.10190)	**qPCR**	MK804	5'-GAG CGT GTG ACT TCC GAA GG-3'	-
		MK805	5'-AGG AAC TGT CAC GGA GTT TGC-3'	-

Appendix B: Supplementary Data

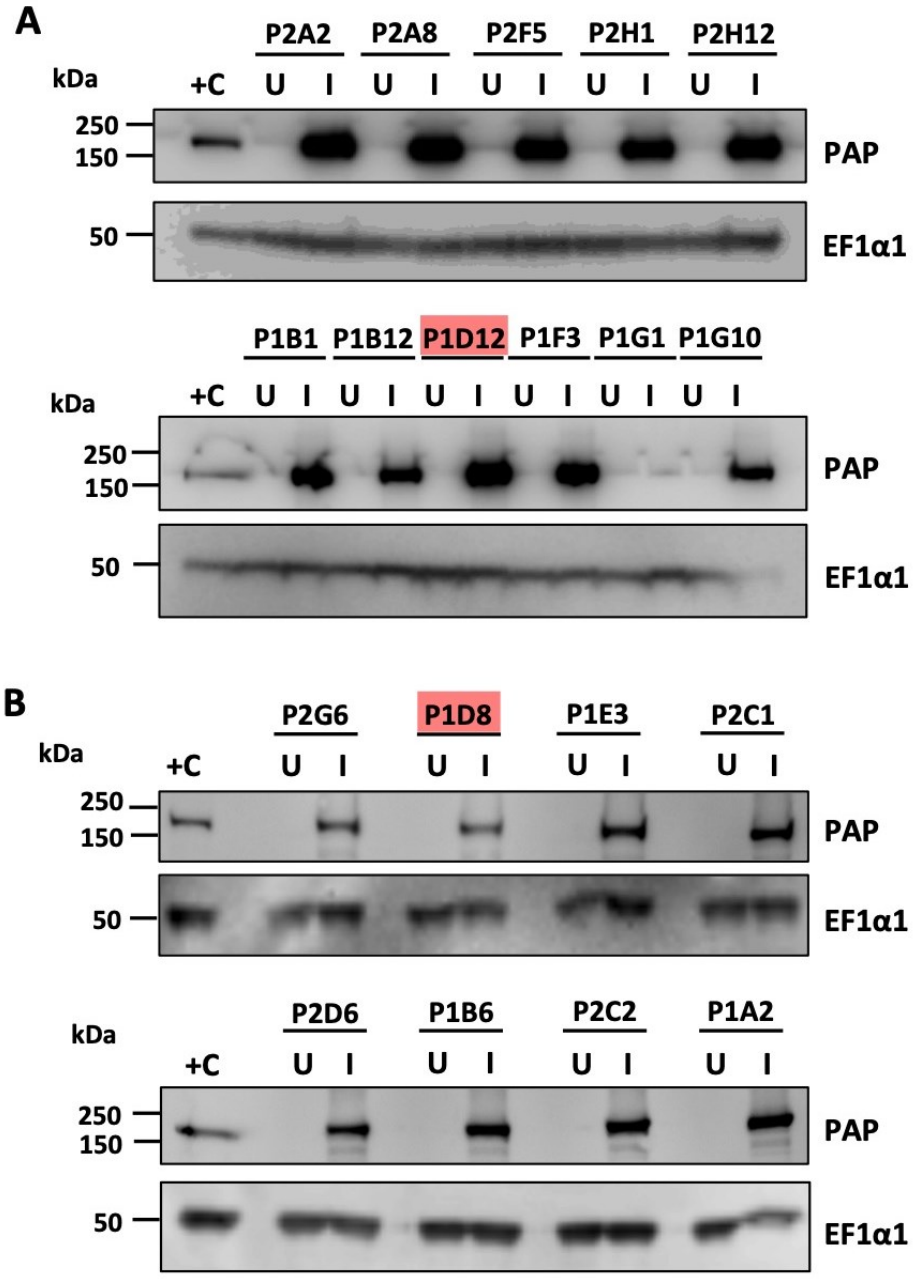

Appendix B1: Analysis of IBWT^{PTP} and IBPol-^{PTP} overexpression in procyclic cells.
Clonal cell lines were induced with 1 µg/ml tetracycline for 2 days to screen for protein expression. Western blot detection of the PTP-tagged variant and EF1α1 from whole cell lysates. A) Screen of 11 IBWT^{PTP} OE clones. 3 x 10^6 cell equivalents were loaded across all lanes. B) Screen of 8 IBPol-^{PTP} OE clones. 1 x 10^6 cell equivalents were loaded into each well except for +C where 5 x 10^6 cell equivalents were loaded. +C, single allele control cell line endogenously expressing POLIB-PTP; U, Uninduced; I, Induced. Clones labeled with red box were selected for further characterization.

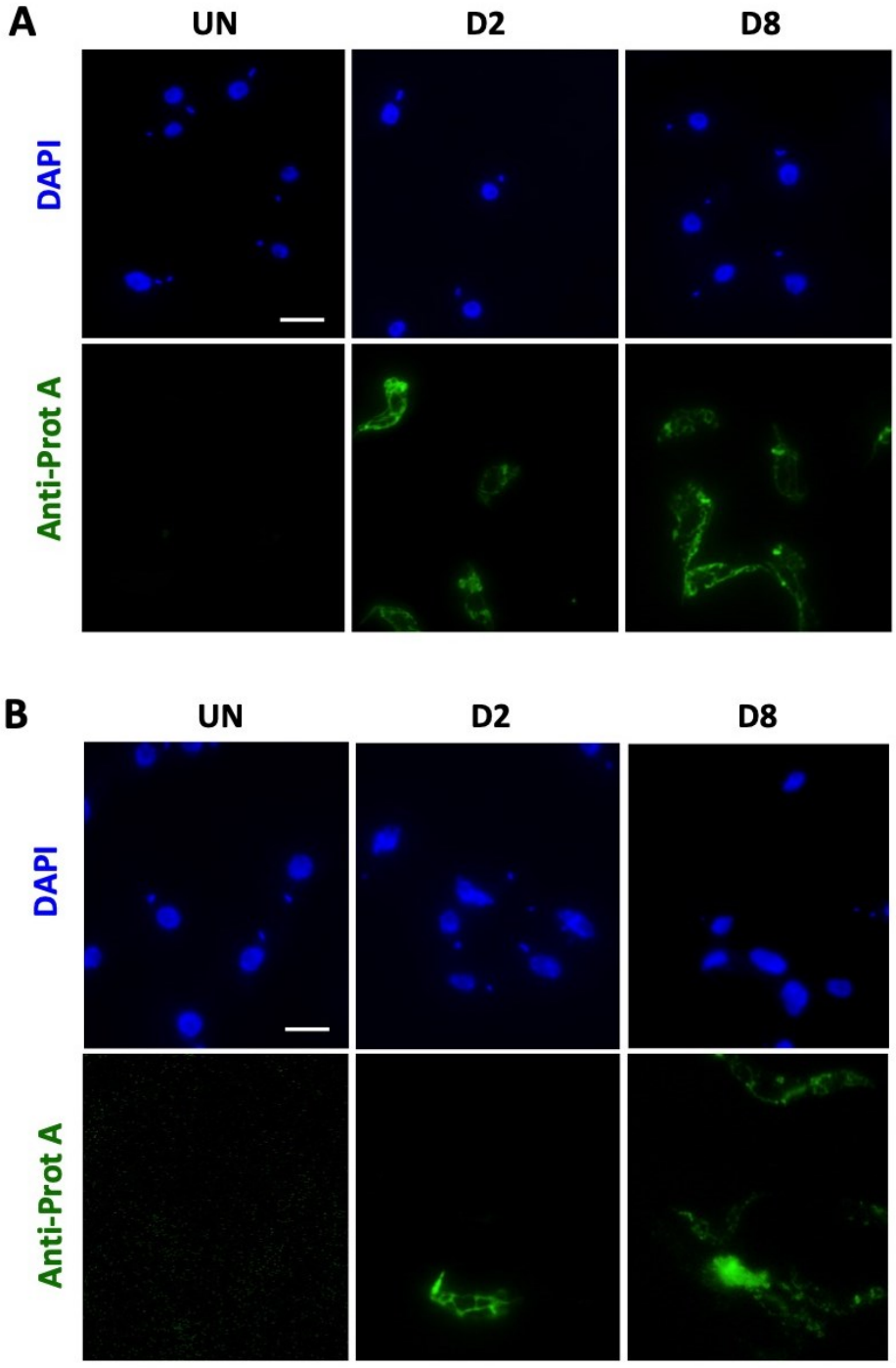

Appendix B2. Expression of IBWT^{PTP} at selected time points.
A) Clonal cell line IBWT^{PTP} OE P1D12 was grown in the absence and presence of 1 µg/ml tetracycline. **B)** Clonal cell line IBRNAi + IBWT^{PTP} P2G7 was grown in the absence and presence of 4 µg/ml tetracycline. Cells were stained/labeled with DAPI (blue) and anti-protein A (green) at the selected time points. Scale bar, 5 µm.

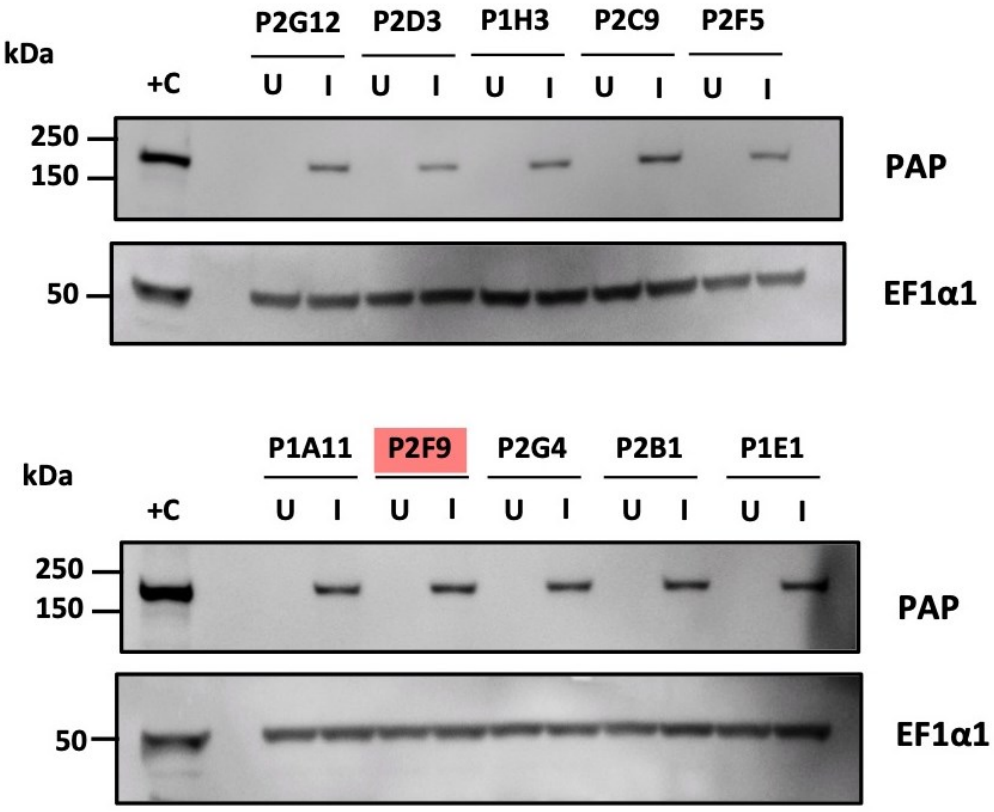

Appendix B3: Dual Induction of *POLIB* RNAi and ectopic expression of IBPol-^{PTP} variant.
Clonal cell lines were induced with 1 μg/ml tetracycline for 2 days to screen for protein expression. Western blot detection of IBWT^{PTP} variant and EF1α1 from whole cell lysates. Screen of 10 IBRNAi + IBPol-^{PTP} clones. +C, single allele control cell line endogenously expressing POLIB-PTP; U, Uninduced; I, Induced. 1 x 10^6 cell equivalents were loaded into each well except for +C where 5 x 10^6 cell equivalents were loaded. Clone labeled with red box was selected for further characterization.

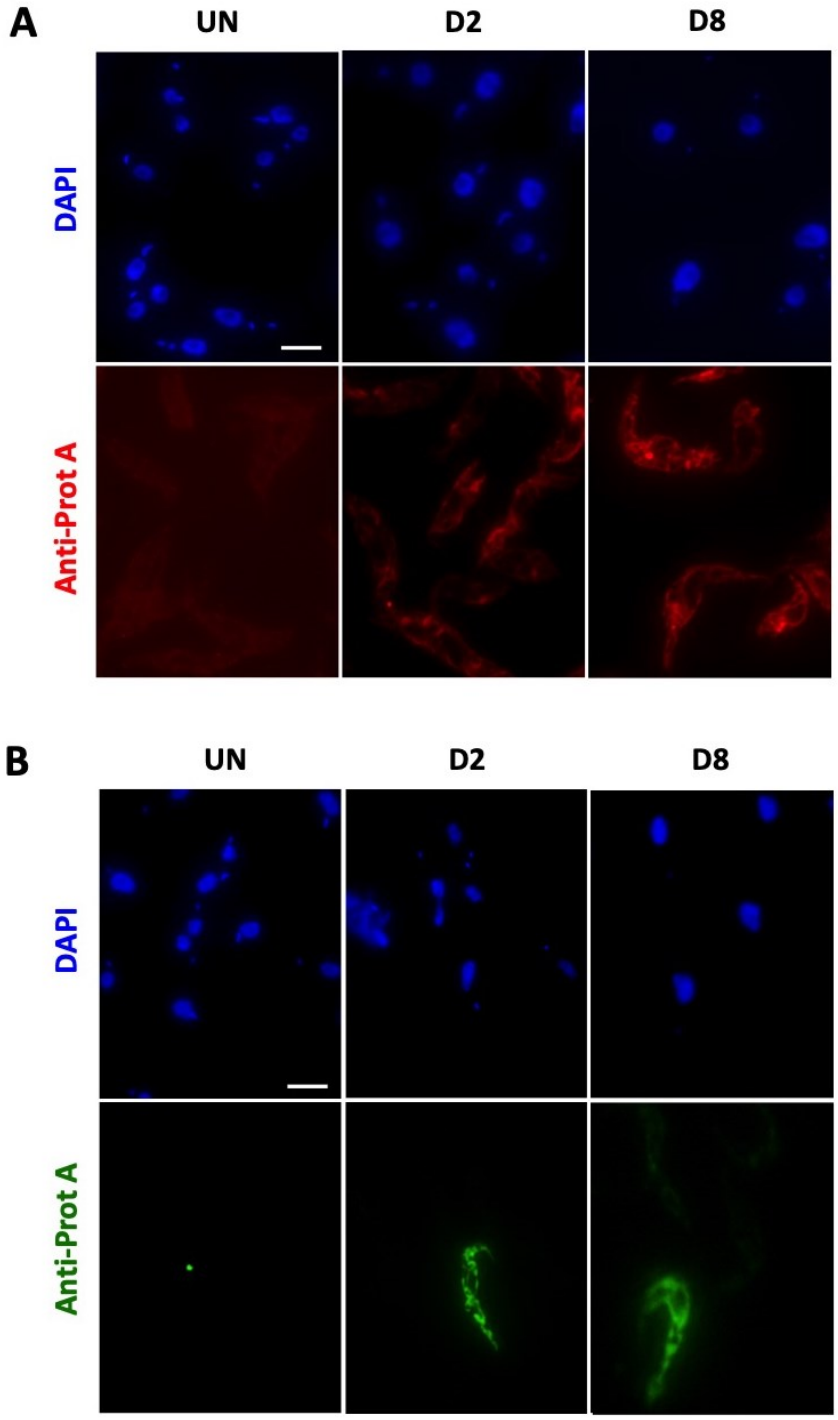

Appendix B4. Expression of IBPol-^{PTP} at selected time points.
A) Clonal cell line IBPol-^{PTP} OE P1D8 was grown in the absence and presence of 1 µg/ml tetracycline. Cells were stained/labeled with DAPI (blue) and anti-protein A (red) at the selected time points. **B)** Clonal cell line IBRNAi + IBPol-^{PTP} P2F9 was grown in the absence and presence of 4 µg/ml tetracycline. Cells were stained/labeled with DAPI (blue) and anti-protein A (green) at the selected time points. Scale bar, 5 µm.

BIBLIOGRAPHY

Baldauf, S. L. (2003). The deep roots of eukaryotes. *Science* **300**, 1703-1706. doi:10.1126/science.1085544

Baral, T. N. (2010). Immunobiology of African trypanosomes: need of alternative interventions. *J Biomed Biotechnol* **2010,** 389153. doi:10.1155/2010/389153

Boelaert, M., Meheus, F., Robays, J., and Lutumba, P. (2010) Socio-economic aspects of neglected diseases: sleeping sickness and visceral leishmaniasis. *Ann Trop Med Parasitol* **104,** 535-542. doi:10.1179/136485910X12786389891641

Brenndörfer, M. and Boshart, M. (2010). Selection of reference genes for mRNA quantification in *Trypanosoma brucei. Mol. Biochem. Parasitol.* **172,** 52-55. doi:10.1016/j.molbiopara.2010.03.007

Bruhn, D. F., Mozeleski, B., Falkin, L. and Klingbeil, M. M. (2010). Mitochondrial DNA polymerase POLIB is essential for minicircle DNA replication in African trypanosomes. *Mol. Microbiol.* **75,** 1414-1425. doi:10.1111/j.1365-2958.2010. 07061.x

Bruhn, D. F., Sammartino, M. P. and Klingbeil, M. M. (2011). Three mitochondrial DNA polymerases are essential for kinetoplast DNA replication and survival of bloodstream form *Trypanosoma brucei*. *Eukaryot. Cell* **10,** 734-743. doi:10.1128/ EC.05008-11

Chandler, J., Vandoros, A. V., Mozeleski, B. and Klingbeil, M. M. (2008). Stemloop silencing reveals that a third mitochondrial DNA polymerase, *POLID*, is required for kinetoplast DNA replication in trypanosomes. *Eukaryot. Cell* **7,** 2141-2146. doi:10.1128/EC.00199-08

Clark, David P., et al. *Molecular Biology*. Academic Press, an Imprint of Elsevier, 2019.
DiMaio, J., Ruthel, G., Cannon, J. J., Malfara, M. F., and Povelones, M. L. (2018). The single mitochondrion of the kinetoplastid parasite *Crithidia fasciculata* is a dynamic network. *PloS One* **13,** e0202711. doi:10.1371/journal.pone.0202711

Corliss, J.O. (1989). Protistan diversity and origins of multicellular/multitissued organisms, *Italian J. Zool.* **56,** 227-234, doi:10.1080/11250008909355646

Davies, C., Ooi, C. P., Sioutas, G., Hall, B. S., Sidhu, H., Butter, F., Alsford, S., Wickstead, B., and Rudenko, G. (2021). *TbSAP* is a novel chromatin protein repressing metacyclic variant surface glycoprotein expression sites in bloodstream form *Trypanosoma brucei*. *Nucleic acids res*, ***49***, 3242–3262. doi:10.1093/nar/gkab109

Drew ME, Englund PT. Intramitochondrial location and dynamics of Crithidia fasciculate kinetoplast minicircle replication intermediates. (2001). *J Cell Biol.* **153,** 735-44. doi: 10.1083/jcb.153.4.735.

Dua, R., Levy, D. L., and Campbell, J. L. (1999). Analysis of the essential functions of the C-terminal protein/protein interaction domain of *Saccharomyces cerevisiae* pol ε and its unexpected ability to support growth in the absence of the DNA polymerase domain. *J. Biol. Chem.* **274**, 22283-22288. doi:10.1074/jbc.274.32. 22283

Dyer, N.A., Rose, C., Ejeh, N.O. and Acosta-Serrano, A. (2013) Flying tryps: survival and maturation of trypanosomes in tsetse flies.*Trends Parasitol.* **29,** 188-96. doi: 10.1016/j.pt.2013.02.003.

Ferguson, M. L., Torri, A. F., Pérez-Morga, D., Ward, D. C., and Englund, P. T. (1994). Kinetoplast DNA replication: mechanistic differences between *Trypanosoma brucei* and *Crithidia fasciculata*. *J. Cell Biol.* **126,** 631–639. doi:10.1083/jcb.126.3.631

Gray, M. (2017). Lynn Margulis and the endosymbiont hypothesis: 50 years later. *Mol. Biol. Cell* **28,** 1285-1287. doi:10.1091/mbc.E16-07-0509

Gull, K. (2002). The cell biology of parasitism in *Trypanosoma brucei*: insights and drug targets from genomic approaches?. *Current Pharm. Design* **8,** 241–256. doi:10.2174/1381612023396212

Hines, J. C., Engel, M. L., Zhao, H., and Ray, D. S. (2001). RNA primer removal and gap filling on a model minicircle replication intermediate. *Mol. Biochem. Parasitol*. **115**, 63–67. doi:10.1016/s0166-6851(01)00272-9

Horn D. (2008). Codon usage suggests that translational selection has a major impact on protein expression in trypanosomatids. *BMC Genomics* **9,** 2. doi: 10.1186/1471-2164-9-2

Hotez, P. J., Bottazzi, M. E., Franco-Paredes, C., Ault, S. K., and Periago, M. R. (2008). The neglected tropical diseases of Latin America and the Caribbean: a review of disease burden and distribution and a roadmap for control and elimination. *PLoS Negl. Trop. Dis.* **2,** e300. doi:10.1371/journal.pntd.0000300

Hotez, P. J., Dumonteil, E., Woc-Colburn, L., Serpa, J. A., Bezek, S., Edwards, M. S., Hallmark, C. J., Musselwhite, L. W., Flink, B. J., and Bottazzi, M. E. (2012). Chagas disease: "the new HIV/AIDS of the Americas". *PLoS Negl. Trop. Dis.* **6,** e1498. doi:10.1371/journal.pntd.0001498

Johnson, K. A., and Rosenbaum, J. L. (1991). Basal bodies and DNA. *Trends Cell Biol*. **1**, 145–149. doi:10.1016/0962-8924(91)90002-q

Käser, S., Oeljeklaus, S., Týč, J., Vaughan, S., Warscheid, B., and Schneider, A. (2016). Outer membrane protein functions as integrator of protein import and DNA inheritance in mitochondria. *Proc. Natl. Acad. Sci. USA* **113**, E4467-E4475. doi:10.1073/pnas.1605497113

Kaufer, A., Stark, D. and Ellis, J. (2020). A review of the systematics, species identification and diagnostics of the Trypabosomatidae using maxicircle kinetoplast DNA: from past to present. *Int. J. Parasitol*. **50,** 449-460. doi: 10.1016/j.ijpara.2020.03.003.

Kesti, T., Flick, K., Keränen, S., Syvä oja, J. E., and Wittenberg, C. (1999). DNA polymerase ε catalytic domains are dispensable for DNA replication, DNA repair, and cell viability. *Mol. Cell* **3**, 679-685. doi:10.1016/S1097-2765(00)80361-5

Klingbeil, M. M., Motyka, S. A., and Englund, P. T. (2002). Multiple mitochondrial DNA polymerases in *Trypanosoma brucei*. *Mol. Cell* **10**, 175–186. doi:10.1016/s1097-2765(02)00571-3

Lukeš, J., Wheeler, R., Jirsová, D., David, V., and Archibald, J. M. (2018). Massive mitochondrial DNA content in diplonemid and kinetoplastid protists. *IUBMB Life*, **70**, 1267-1274. doi:10.1002/iub.1894

Melendy, T., Sheline, C., and Ray, D. S. (1988). Localization of a type II DNA topoisomerase to two sites at the periphery of the kinetoplast DNA of *Crithidia fasciculata*. *Cell* **55**, 1083–1088. doi:10.1016/0092-8674(88)90252-8

Miller, J. C., Delzell, S. B., Concepción-Acevedo, J., Boucher, M. J., Klingbeil, M. M. (2020). A DNA polymerization-independent role for mitochondrial DNA polymerase I-like protein C in African trypanosomes. *J Cell Sci*. **133**:jcs233072. doi: 10.1242/jcs.233072

Moriyama, T., Terasawa, K., and Sato, N. (2011). Conservation of POPs, the plant organellar DNA polymerases, in eukaryotes. *Protist* **162**, 177–187. doi:10.1016/j.protis.2010.06.001

Njiokou, F., Laveissière, C., Simo, G., Nkinin, S., Grébaut, P., Cuny, G., and Herder, S. (2006). Wild fauna as a probable animal reservoir for *Trypanosoma brucei gambiense* in Cameroon. *MEEGID* **6**, 147–153. doi:10.1016/j.meegid.2005.04.003

Rusconi, F., Durand-Dubief, M. and Bastin, P. (2005). Functional complementation of RNA interference mutants in trypanosomes. *BMC Biotechnol*. **5**, 6. doi:10.1186/1472-6750-5-6

Ralston, K. S., Kisalu, N. K. and Hill, K. L. (2011). Structure-function analysis of dynein light chain 1 identifies viable motility mutants in bloodstream-form *Trypanosoma brucei*. *Eukaryot. Cell* **10**, 884-894. doi:10.1128/EC.00298-10

Raper, J., Fung, R., Ghiso, J., Nussenzweig, V., and Tomlinson, S. (1999). Characterization of a novel trypanosome lytic factor from human serum. *Infect. Immun* **67**, 1910–1916. doi:10.1128/IAI.67.4.1910-1916.1999

Rusconi, F., Durand-Dubief, M., and Bastin, P. (2005). Functional complementation of RNA interference mutants in trypanosomes. *BMC Biotechnol,* ***5***, 6. doi:10.1186/1472-6750-5-6

Sagan, L. (1967). On the origin of mitosing cells. *J. Theor. Biol.* **14**, 225-IN6. doi:10.1016/0022-5193(67)90079-3

Saxowsky, T. T., Choudhary, G., Klingbeil, M. M., and Englund, P. T. (2003). *Trypanosoma brucei* has two distinct mitochondrial DNA polymerase beta enzymes. *J. Biol. Chem.* **278**, 49095–49101. doi:10.1074/jbc.M308565200

Schmid, C., Nkunku, S., Merolle, A., Vounatsou, P., and Burri, C. (2004). Efficacy of 10-day melarsoprol schedule 2 years after treatment for late-stage *gambiense* sleeping sickness. *Lancet* **364**, 789–790. doi:10.1016/S0140-6736(04)16940-7

Scocca, J. R., and Shapiro, T. A. (2008). A mitochondrial topoisomerase IA essential for late theta structure resolution in African trypanosomes. *Mol. Microbiol* **67**, 820–829. doi:10.1111/j.1365-2958.2007.06087.x

Shlomai J. (2004). The structure and replication of kinetoplast DNA. *Curr. Mol. Med* **4**, 623–647. doi:10.2174/1566524043360096

Simo, G., Asonganyi, T., Nkinin, S. W., Njiokou, F., and Herder, S. (2006). High prevalence of *Trypanosoma brucei gambiense* group 1 in pigs from the Fontem sleeping sickness focus in Cameroon. *Vet. Parasitol.* **139,** 57–66. doi:10.1016/j.vetpar.2006.02.026

Sunter J. D. (2016). A vanillic acid inducible expression system for *Trypanosoma brucei*. *Mol. Biochem. Parasitol*. ***207***, 45–48. doi:10.1016/j.molbiopara.2016.04.001

Trikin, R., Doiron, N., Hoffmann, A., Haenni, B., Jakob, M., Schnaufer, A., Schimanski, B., Zuber, B. and Ochsenreiter, T. (2016). *TAC102* is a novel component of the mitochondrial genome segregation machinery in trypanosomes. *PLoS Pathog.* **12,** e1005586. doi:10.1371/journal.ppat.1005586

Weems, E., Singha, U. K., Hamilton, V., Smith, J. T., Waegemann, K., Mokranjac, D. and Chaudhuri, M. (2015). Functional complementation analyses reveal that the single PRAT family protein of

Trypanosoma brucei is a divergent homolog of *Tim17* in Saccharomyces cerevisiae. *Eukaryot. Cell* **14,** 286-296. doi:10.1128/EC.00203-14

Whelan, S. P., and Zuckerbraun, B. S. (2013). Mitochondrial signaling: forwards, backwards, and in between. *Oxid. Med. Cell. Longev.* ***2013*****,** 351613. doi:10.1155/2013/351613

Wickstead, B., Ersfeld, K. and Gull, K. (2003). The frequency of gene targeting in *Trypanosoma brucei* is independent of target site copy number. *Nucl. Acids Res.* **31,** 3993-4000.

Wirtz, E., Leal, S., Ochatt, C. and Cross, G. M. (1999). A tightly regulated inducible expression system for conditional gene knock-outs and dominant-negative genetics in *Trypanosoma brucei*. *Mol. Biochem. Parasitol*. **99**, 89-101. doi:10.1016/S0166-6851(99)00002-X

Woodward, R., and Gull, K. (1990). Timing of nuclear and kinetoplast DNA replication and early morphological events in the cell cycle of *Trypanosoma brucei. J. Cell Sci.* **95,** 49–57.

Yu, Z., Liu, Y. and Li, Z. (2012). Structure–function relationship of the Polo-like kinase in *Trypanosoma brucei*. *J. Cell Sci*. **125**, 1519-1530. doi:10.1242/jcs.094243